AIR FORCE INSTITUTE OF TECHNOLOGY

AIR UNIVERSITY
UNITED STATES AIR FORCE

SCHOOL OF ENGINEERING

WRIGHT-PATTERSON AIR FORCE BASE, OHIO

AF-WP-O-MAY 62 3,500

AN EVALUATION OF AN EXPERIMENTAL LASER RANGING SYSTEM

Alton B. Todd

GA/EE/62-4

EVALUATION OF AN EXPERIMENTAL LASER RANGING SYSTEM

THESIS

Presented to the Faculty of the School of Engineering

of the Air Force Institute of Technology

Air University

in Partial Fulfillment of the

Requirements for the Degree of

Master of Science

By

Alton B. Todd, B.E.E.

Graduate Astronautics

August 1962

Preface

The Navigation and Guidance Laboratory, ASD, wished to conduct an independent experiment in the construction and evaluation of a simple LASER ranging system to determine first hand the performance to be expected of a system operating in the atmosphere, to evaluate the particular design adopted and to gain experience on the operating characteristics of LASERs. When I took over the project, most of the basic mechanical and optical construction was completed, although numerous modifications and additions were made during the course of the work. My contributions to the equipment were design of the preamplifier, the trigger pickoff unit and the trigger amplifier plus design of a large number of mechanical bits and pieces required to make a workable system. I also debugged and made the device operative, focused it and aligned it.

In looking around for theoretical work on which to base a prediction of the performance of the system, I was fortunate to find that people at Hughes Aircraft Company had done some work of this kind. I made free use of their work but incorporated modifications and interpretations of my own. For that reason any errors in the derivations and interpretations given are probably not attributable to Hughes.

It was the intent to experimentally determine the signal-to-noise-ratio versus range of the system as a measure of its per-

formance and compare this with values predicted. This was done except that a non-experimentally determined value of atmospheric attenuation was included in the result to make the results more useful, in my opinion. The experimental data is, unfortunately, skimpy in some areas because of time limitations. Repeated breakdowns of the LASER equipment prevented any serious data taking until less than three weeks before the deadline for this report.

I wish to acknowledge the continued help and cooperation of Mr. Janis Sirons, my ASD sponsor, who supported me beyond the call of duty on several critical occasions. I also wish to acknowledge the support of Mr. Jerry Pasek who provided the use of laboratory facilities and personnel throughout the project. Mr. George Helentjaris, the laboratory technician, did an outstanding job on building up circuits and in helping me on numerous jobs ranging from assembling equipment to lifting heavy objects. Many thanks to Major Everette T. Garrett, my faculty thesis advisor, for his advice and encouragement.

Contents

Page

List of Figures

Figure Page

Figure Page

Abstract

A simple LASER ranging system was built and experimentally evaluated regarding signal-to-noise-ratio versus range attainable. The transmitter consists of a Technical Research Group Model V-2909 commercial LASER equipment and a collimator to reduce the beamwidth. The receiver consists of a 36" parabolic mirror focused on an RCA 7265 photomultiplier. The dominant sources of noise in the system are background sunlight and backscattering of LASER energy. Measurement of interference due to sunlight for targets of high reflectance shows a slightly decreasing value with range which agrees with theory presented, but a general level 8 db higher than predicted. Measurements of backscattering received show the characteristic rapid buildup and leveling off with range predicted by the theory and a very comparable magnitude. Return signal strength versus range was determined by extrapolation of measurements on one target. This was compared with the sum of the two dominant noise sources to obtain signal-to-noise-ratio. Measured signal-to-noise-ratio thus obtained compares favorably with the predicted value except for a greater day-night difference resulting from the greater than predicted sunlight interference.

EVALUATION OF AN EXPERIMENTAL LASER RANGING SYSTEM

I. Introduction

The purpose of the project described in this report was to complete the design and construction of a rudimentary LASER optical ranging system, which was under construction by the sponsoring Laboratory, and to evaluate its performance, mainly regarding signal-to-noise-ratio as a function or range; and to compare this with predicted performance. The well publicized (Ref 5) advantages of a LASER as a light source for optical ranging are chiefly its large spectral radiance and its potentially narrow beamwidth. The energy output of the ruby LASER is concentrated in a band approximately 0.1 $\mathring{A}$ wide centered at 6943 $\mathring{A}$. This feature allows the filtering out of background sunlight or other interfering sources of light to a very great extent. The power output of the LASER is not enormous, being of the order of 500 watts average during the approximately 500 microsecond output period but this power is directed in a beam of nominally 10 milliradians width so that the intensity of the beam is 2×10^7 watts per steradian. By the use of simple optics the beam can be narrowed to one milliradian or less resulting in an intensity of 2×10^9 watts per steradian, which is comparable to that obtained in high powered radar systems. The very narrow beam width of the LASER system gives the added advantage of very

high angular resolution.

For the system under consideration the general scheme of operation is to transmit a burst of light energy and observe the time delay incurred by the signal in traversing the distance from the transmitter to the target and back. Contrary to the case of a conventional microwave radar, the energy output of the LASER used in the system is not concentrated in a single pulse but rather the output consists of a long train of randomly spaced pulses of random amplitude. Figure 1 shows the appearance of the power waveform using two different oscilloscope sweep speeds. Figure 1a shows the

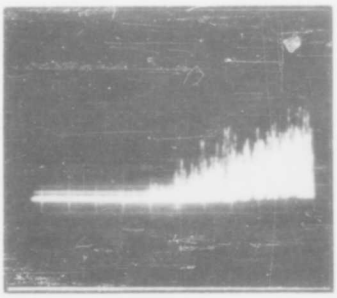

(a) Horizontal Scale 100 usec./div.

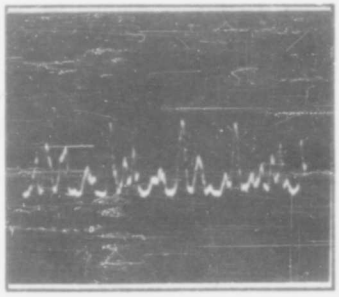

(b) Horizontal Scale 2 usec./div.

Fig. 1

The LASER Output Waveform

entire burst of energy. The output begins on the right hand side of the scale and continues for something over 500 microseconds. Figure 1b is an expanded portion of the output burst. The discrete

output pulses are readily seen. The pulse length of the individual pulses is of the order of 0.5 microsecond. To measure the time delay of the echo in the system one may trigger the receiver oscilloscope sweep at the initial output pulse of the LASER and observe the shift in time of the return signal. An alternative method is to present the transmitted and received waveforms on a dual beam oscilloscope or on two separate but synchronized oscilloscopes and observe the relative shift in position of corresponding identifiable features of the waveforms. Both of these methods were used during the experiment.

II. Description of the System

Figure 2 is a block diagram of the system. Essentially, the transmitter consists of the LASER and its collimator, and the receiver consists of a 36 inch parabolic mirror focused on the cathode of an RCA 7265 photomultiplier tube. When the LASER is fired, part of its energy is reflected off the target and returns to the receiver where an oscilloscope presentation of the amplitude envelope of the reflected light is made. The oscilloscope sweep is triggered at the time of the first detectable output pulse from the LASER by means of the trigger pickoff unit which contains a photoelectric cell that detects the transmitted envelope. This trigger signal is recorded by a second oscilloscope in an alternate mode of operation where the range is determined by comparison of the transmitted and received envelopes, i.e., by the shift in time of one relative to the other. Figures 3 and 4 are front and rear views of the system. The key components of the system are identified by the number pointers as follows:

1 - the detector head including the photomultiplier, field stop selector, optical filter, lens, dynode voltage divider network and preamplifier

2 - 36" receiving mirror

3 - the output end of the transmitter collimator

4 - telescope used to point the system

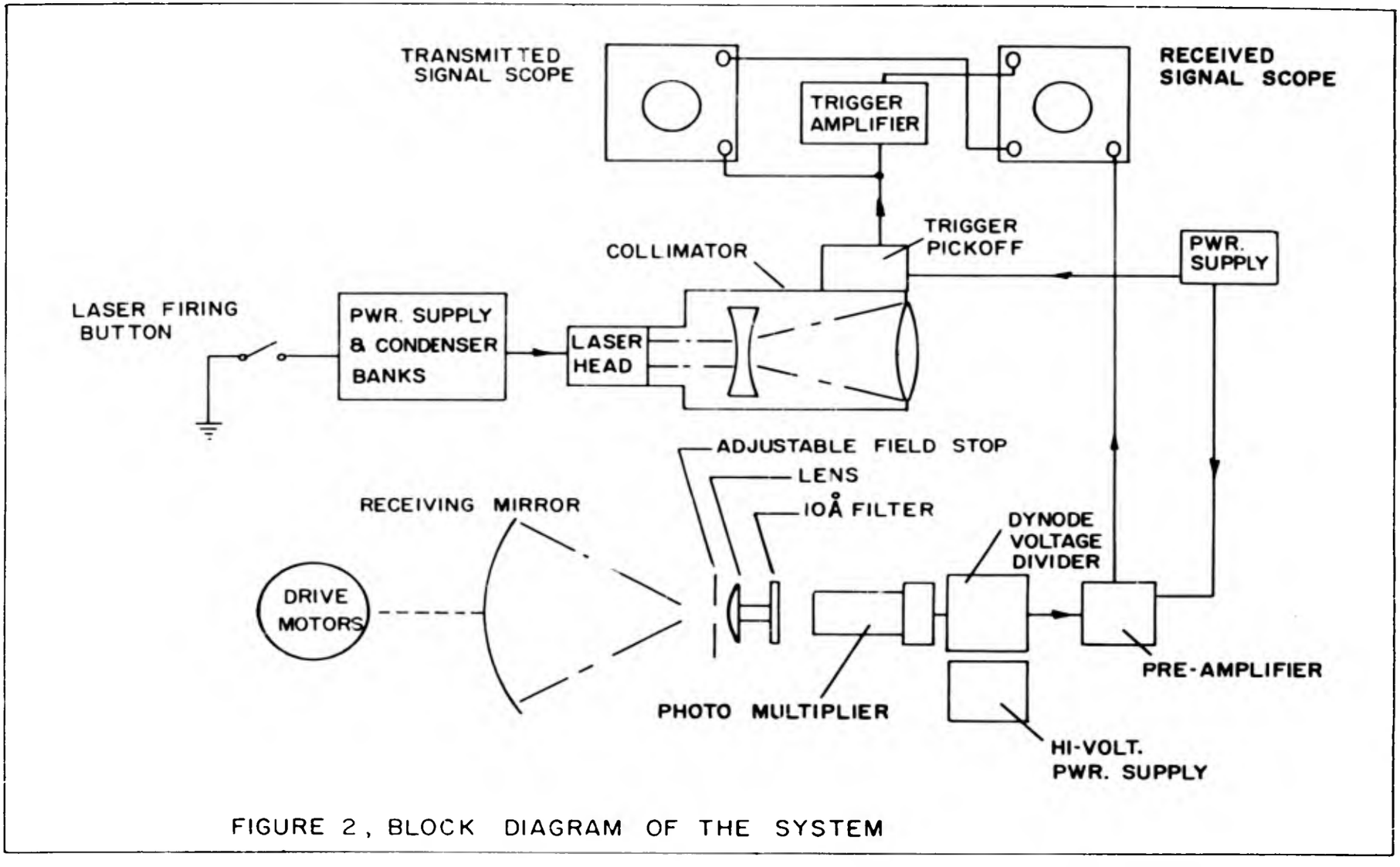

FIGURE 2, BLOCK DIAGRAM OF THE SYSTEM

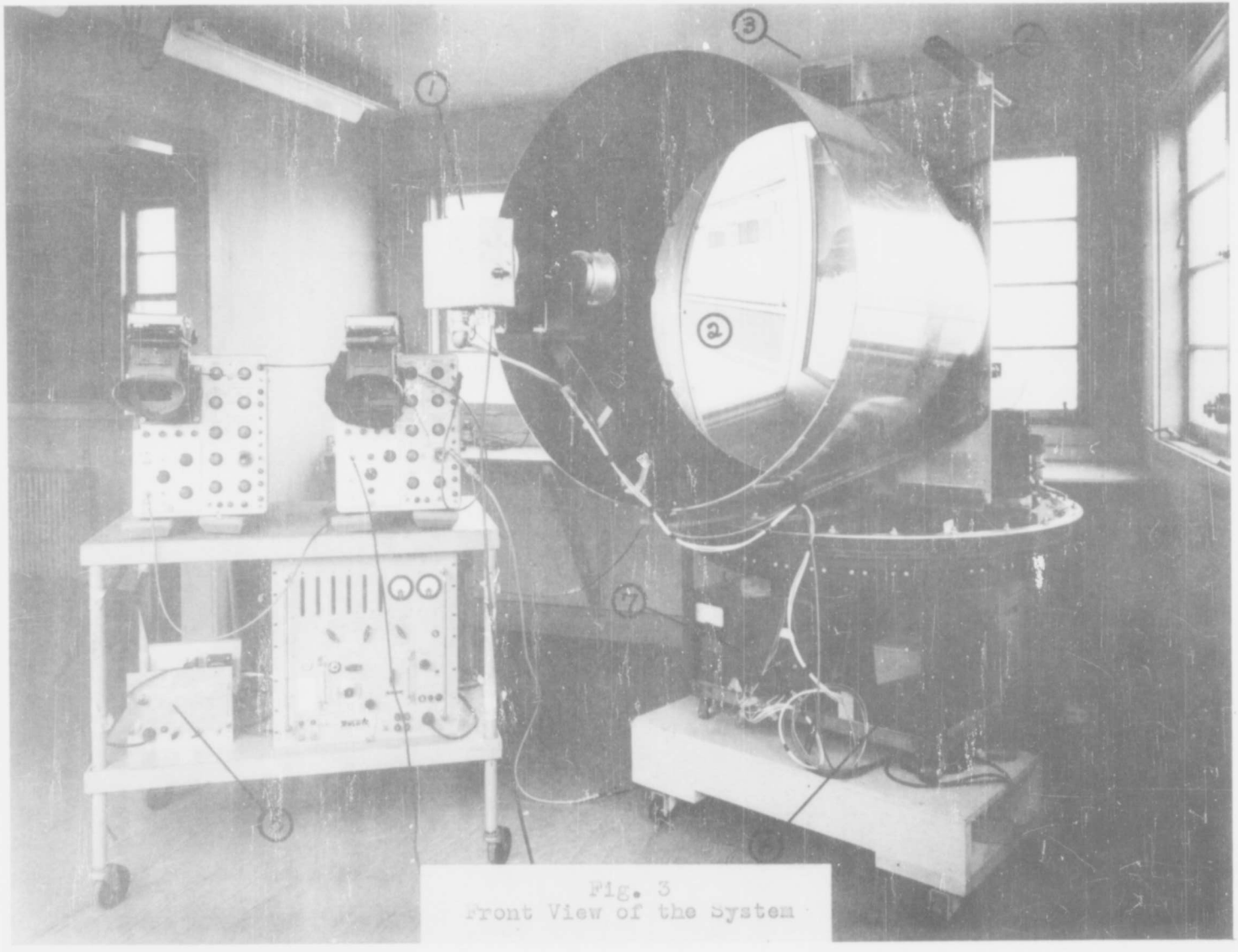

Fig. 3
Front View of the System

Fig. 4
Rear View of the system

5 - trigger amplifier

6 - high voltage power supply for photomultiplier

7 - power supply for preamplifier and trigger pickoff unit

8 - LASER power supply and condenser bank unit

9 - collimator

10 - LASER head containing ruby rod and flash tubes

11 - trigger pickoff unit

As may be seen in the photographs the components are mounted on a modified aircraft gun mount which provides rotation in azimuth and elevation of the upper portion of the assembly relative to the lower portion, for purposes of pointing at a target. The entire assembly was moved in front of the appropriate window of the building by rolling it on the casters shown.

Details of the Transmitter

The LASER. The LASER is a commercial equipment (Technical Research Group Model V2909) consisting of the LASER head and a power supply-energy storage unit. The LASER head contains a ruby rod approximately seven centimeters long and one centimeter in diameter. The ruby rod is surrounded by four Xenon filled gas discharge flash tubes which furnish the pumping energy for the LASER.

The power supply contains four separate banks of electrolytic capacitors of 550 microfarads per bank. These may be charged to a maximum of 950 volts for a total energy storage of slightly over

1000 joules. The power supply unit also houses circuits which provide a pulse of current to each of four sparking coils in the LASER head which have the purpose of providing the ionizing potential to flash the tubes.

Collimator. The collimator is essentially a Gallilean telescope with the LASER output aperture located where an observer's eye would normally be. Its purpose is to provide narrowing of the LASER beam below its natural beamwidth of about 10 milliradians. The Gallilean telescope uses a negative ocular lens as opposed to the astronomical telescope which uses a positive ocular (Ref 7:149). The principle advantage of the Gallilean type is that the overall length of the telescope is less than for the astronomical type. This is due to the fact that in the former the ocular is placed inside the focal length of the objective by an amount equal to the focal length of the ocular whereas in the astronomical telescope, the ocular is outside by the same amount. Figure 5 is a sketch of the essential features of the collimator. Narrowing of the laser beam results from

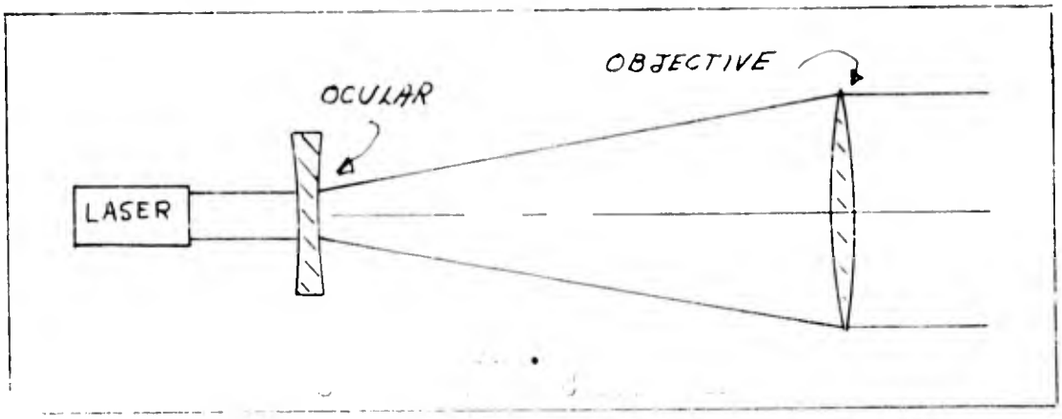

the angular demagnification of the telescope when used in reverse. If f_1 and f_2 are the focal lengths of the objective and ocular, respectively, then the angular demagnification of the telescope is f_2/f_1. In the case at hand, f_1 =50 centimeters and f_2 =10 centimeters so that f_2/f_1 =0.2 and therefore the beamwidth of the output beam is 2 milliradians.

Details of the Receiver

The receiver collector is a 36 inch, f/1 parabolic mirror which forms an image of the target near the photocathode of an RCA 7265 photomultiplier. This image is actually formed in a plane in front of the cathode by approximately two inches. In this plane is a Waterhouse type adjustable field stop having circular apertures equivalent to 0.13, 0.5, 0.9, and 2.0 milliradians field of view. Just behind the field stop is a simple plano-convex lens which serves to converge the rays from the mirror toward the photocathode. Between this lens and the cathode, there is a narrow-band optical filter to stop incoming light except that at the LASER wavelength. The filter is nominally 10 Å wide centered at 6943 Å and has a center transmission of 55 percent.

Photomultiplier. The RCA 7265 photomultiplier is a 14 stage head-on, flat face type having a nominal radiant sensitivity at 6943 Å of 0.12 amperes per microwatt with a 2400 watt power supply. Its current amplification is nominally 9.35×10^6 and its spectral response is S-20.

Preamplifier. The signal at the photomultiplier anode is passed through a two stage vacuum tube preamplifier consisting of a single type 6U8A. The pentode section provides a voltage gain of ten with a high frequency rolloff of five megacycles. The triode section is used as a cathode follower output stage with a gain of 0.85 and an output impedance of approximately 200 ohms. The primary purpose of the preamplifier is to prevent loss of bandwidth due to cable capacitance and other stray capacitance with the consequent loss of detail in the echo signal. The gain of 10 in the pentode was employed to improve the capability to observe the smaller dark current pulses when desired. For normal operation of the system the cathode follower would suffice, because of the tremendous gain of the photomultiplier. Figure 6 is a schematic diagram of the preamplifier. The resistors shown connected to SW-2 are the choice of anode load resistors for the photomultiplier. This resistance was used as one means of controlling the overall gain of the system and is referred to in later sections as R_{Lp}.

Trigger Pickup Unit. The function of the trigger pickup unit is to detect and provide as an electrical signal the transmitted waveform either for triggering the receiving oscilloscope sweep or for recording on the second oscilloscope. The LASER light output is sampled by a photoelectric cell and preamplifier mounted on the back of the collimator assembly. A piece of ordinary kite string is strung

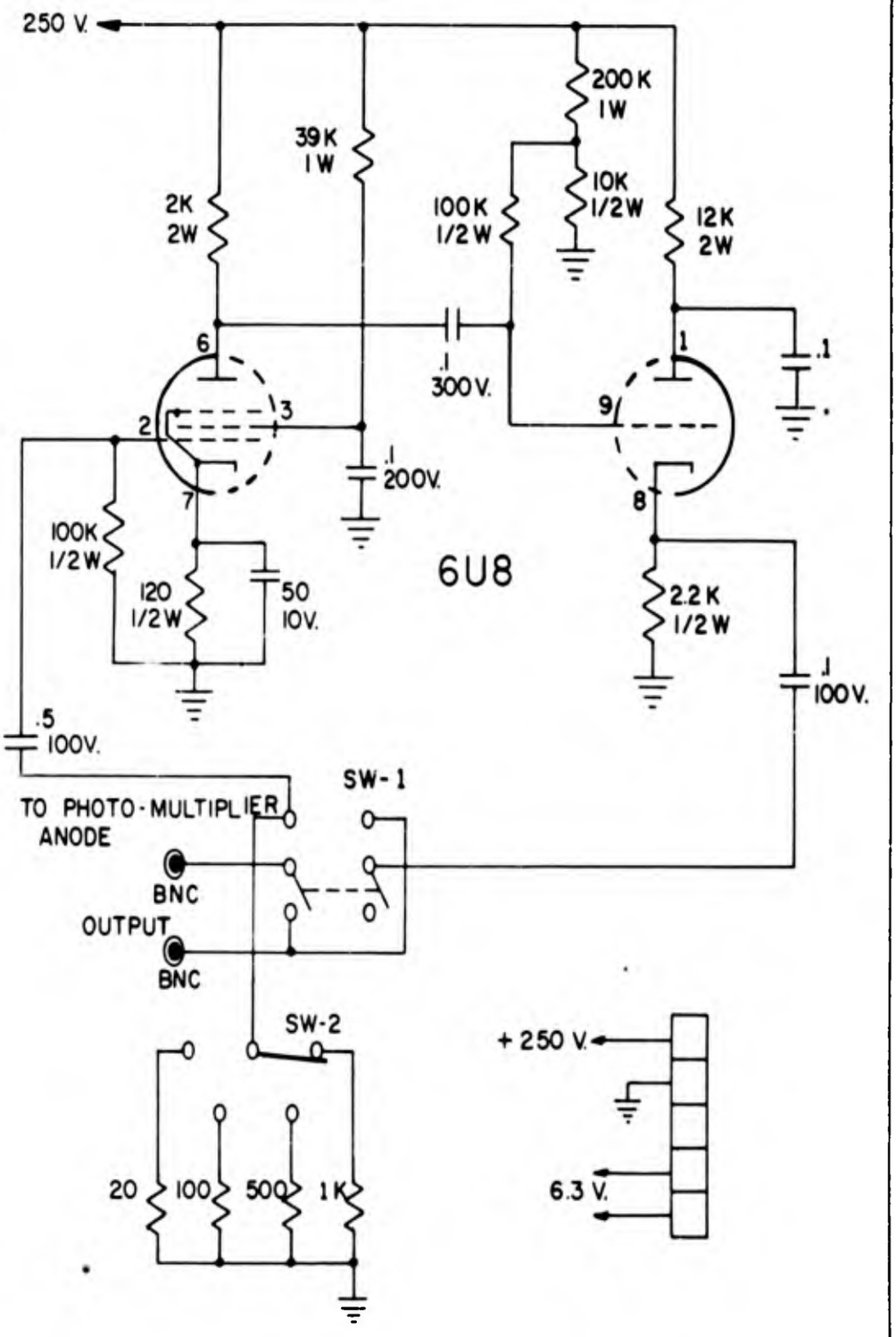

FIGURE 6, SCHEMATIC DIAGRAM OF THE PREAMPLIFIER

diagonally through the light beam between the lenses of the collimator in a region near the objective lens where the beam has been spread out to a diameter of about 1 1/2 inches. The string scatters a small part of the light into an opening in the side of the collimator body and onto the cathode of an RCA 917 vacuum phototube. The phototube output is amplified by a preamplifier similar to the one following the 7265 photomultiplier. Originally this unit was designed only for the purpose of triggering the receiving oscilloscope sweep at the time of the first output pulse from the LASER and so was not designed to have the high frequency response necessary to faithfully reproduce the LASER output waveform. When it became apparent that it would be valuable to record the transmitted waveform simultaneously with the received waveform, the unit was modified by lowering the photocell and pentode load resistances to increase the bandwidth. To offset the loss in gain an external trigger amplifier was added between the unit and the oscilloscope trigger input. A schematic of the trigger pickup unit is shown in Figure 7.

Operating Variables of the System

The three main adjustable parameters of the system are ω, the field stop, R_{Lp}, the photomultiplier anode load resistance, and the oscilloscope gain control. Proper settings of ω and R_{Lp} are necessary to avoid clipping of the return signal by the preamplifier and also in the case of ω, to avoid damage to the photomultiplier tube.

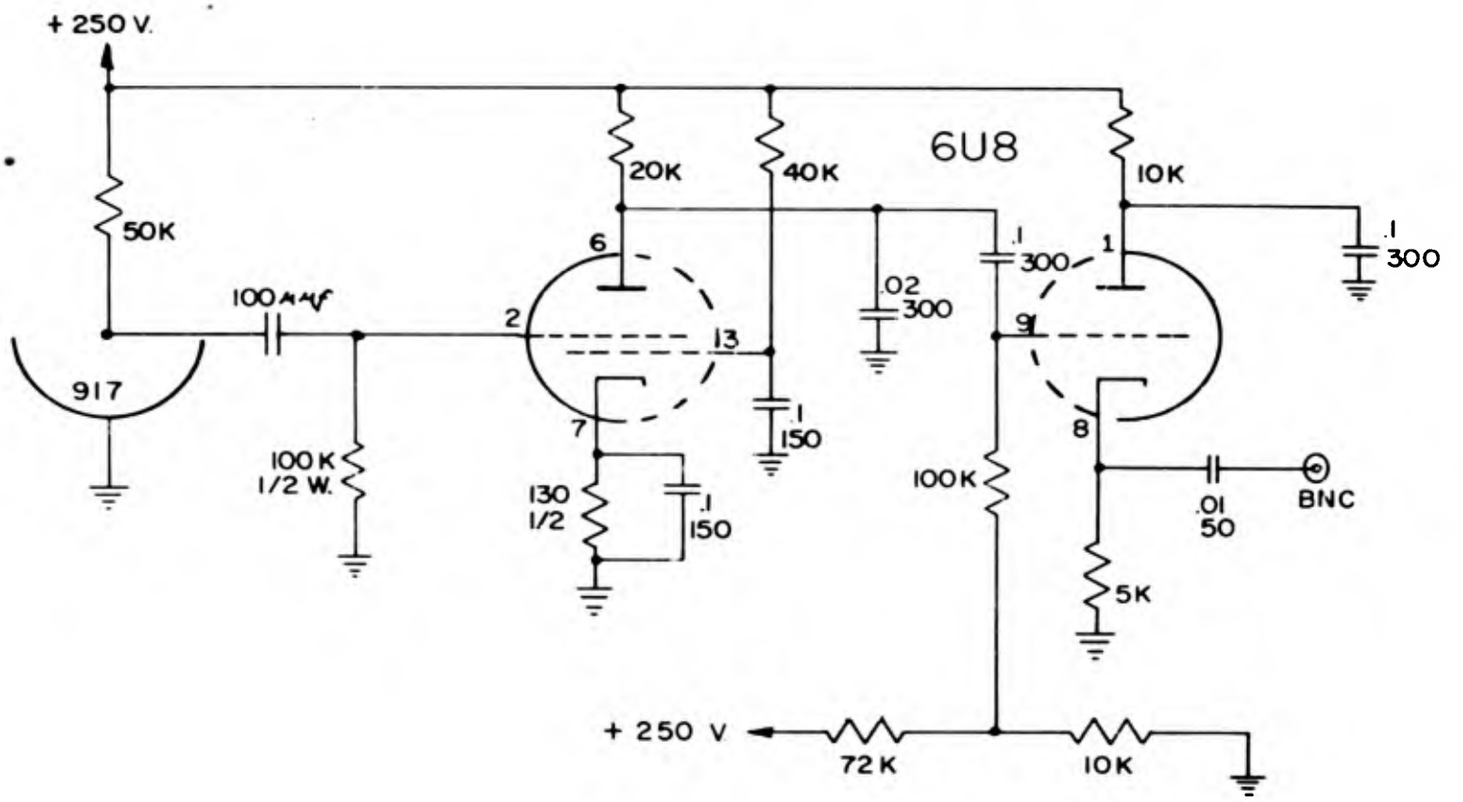

FIGURE 7, SCHEMATIC DIAGRAM OF THE TRIGGER PICKUP UNIT

There is no way incorporated in the system at present to change the sensitivity of the 7265 itself. Therefore, in order not to damage the tube in the daytime by causing excessive anode current to flow, the smallest of the available field stops was used. Even at night, it was necessary to use the smallest ω on close-in targets to prevent overloading of the preamplifier and resultant clipping. The approximate relationships between ω, R_{Lp} and output signal voltage as a function of target range for operation at night may be determined from Figure 26. In general, a combination of R_{Lp} and ω must be chosen to yield an output voltage less than 20 volts to prevent preamplifier overloading. In Figure 26 output voltages for only two values of R_{Lp} are shown because these were the only two used in practice when ranging on targets.

III. Prediction of Performance

To predict the performance of the system, the performance in the absence of interference and atmospheric attenuation was first determined. The effect of atmospheric attenuation on the performance was then considered. Next the sources of interference were investigated and their magnitudes determined. Signal-to-noise ratio was then deduced on the basis of these considerations. Most of the ideas and derivations to do with the sources of interference are due to Smith and Stitch (Ref 8) and Meyers (Ref 3).

Performance Without Interference or Attenuation

Since the beamwidth of the LASER is quite small, it is valid to assume that all the targets that will be used in the experiment completely intercept the transmitted beam. In this case the peak received power in terms of the basic system parameters is (See Appendix A for derivation)

$$P_r = \frac{P_t n_t n_r D^2 \rho \cos\theta}{4R^2} \frac{(\omega)^2}{(\gamma)^2} \quad \omega \leq \gamma \qquad (1)$$

where P_t = the peak transmitted power

n_t = the efficiency of the transmitting optics

n_r = the efficiency of the receiving optics

D = the diameter of the receiving aperture

ρ = the reflectance of the target

θ = the angle at the target between a perpendicular to the

target and the direction of the ranging system

ω = the receiver field of view

γ = the beamwidth of the transmitter

R = distance to target

This expression is based on the assumption that the target is a diffuse reflector, i.e., one for which the intensity of radiation due to it at a distant point is independent of the direction. Let it be assumed that $n_t\ n_r = 0.3$, (the loss occuring mainly in the optical filter which has a center transmission of 0.55), and that $\theta = 0$. As has been previously determined γ is approximately 2 milliradians based on a nominal LASER beamwidth and a collimator power of five. The 36 inch receiving mirror was used during the experiments stopped-down to a diameter of 24 inches because of suspected diminishing advantage of the larger aperture due to aberrations which resulted in poor imaging of the target, and increased scattering of extraneous light into the detector. Regarding the average peak power output of the LASER, a nominal value is derived on the following basis. The maximum energy output as determined by the manufacturer of the LASER is approximately 0.6 joule. Although it is difficult to ascertain precisely, the equipment was operated well below the maximum-approximately halfway between the threshold and maximum, so that a 0.3 joule output is assumed. The output burst lasts for approximately 500 microseconds. Typically, the LASER pulses are

approximately 1 microsecond long and spaced 3 microseconds apart. This may be verified qualitatively by referring to Figure 1b on page 2 which shows a representative portion of the LASER waveform. The above assumptions yield a peak power output of 1800 watts. The last variable in the equation is target reflection coefficient. Reference 1, pages 6-41 gives a value of 0.76 for white lead paint at 6000 Å and 0.79 at 9500 Å. On this basis a value of 0.75 is taken as a conservative estimate for the white squares on two of the water tanks that will be used for targets. With all the above numerical values inserted into (1) it becomes

$$P_r = \frac{101\,\omega^2}{R^2} \tag{2}$$

where ω is in milliradians and R is in feet. To predict the oscilloscope deflection on peaks, the following relation is used:

$$E = P_r\, S_p\, R_{Lp}\, A \tag{3}$$

where S_p = sensitivity of the photomultiplier

R_{Lp} = the anode load resistance of the photomultiplier

A = the voltage gain of the preamplifier

For the type 7265, the nominal value of S_p at 6943 Å is 120,000 amperes/watt. The preamplifier gain is 9. Substituting these values into (3) and combining (2) and (3) the following expression is obtained for the oscilloscope input voltage in terms of the operating variables:

$$E = 1.09 \times 10^8 \frac{R_{Lp} \omega^2}{R^2} \quad (4)$$

Figure 8 shows equations (2) and (4) plotted for the four available values of ω and the two most used values of R_{Lp}.

Attenuation of the LASER Beam

When operating through the atmosphere, the LASER beam is attenuated by scattering of its energy by the atmosphere. At low altitudes this scattering is due primarily to particles such as water vapor, dust, smoke, clouds and the like (Ref 8:17). Figure 9 gives the attenuation to be expected as a function of range and meteorological visibility. The data for this plot was taken from a graph appearing in Reference 8. The meteorological visibility is defined as that distance at which a large dark object is barely discernable against the daylight horizon. Figure 10 shows the predicted peak signal power for a field of view of 1 milliradian when the atmospheric attenuation data is applied to the unattenuated prediction. This plot may be applied to the actual field of view being considered by multiplying the ordinate by the square of the actual field of view.

Sources of Noise

The only sources of interference or noise considered are spurious light inputs to the photomultiplier, and the photomultiplier dark current. The significant sources of spurious light input are background light and backscattering of the LASER beam by the atmo-

Predicted Received Power Neglecting Atmospheric Attenuation
Fig. 8
Range (feet)
1000
10000
100000
ω = 2 mr
ω = 0.9 mr
ω = 0.5 mr
ω = 0.13 mr
E_t = 1600 watts
η_{ant} = 0.5
η_p = 0.75
Received Power (watts)
10^{-4}
10^{-5}
10^{-6}
10^{-7}
10^{-8}
10^{-9}
Peak Receiver Output Voltage
100
80
10-2
10-1-50-
1-1-5-
0.1-0.5-

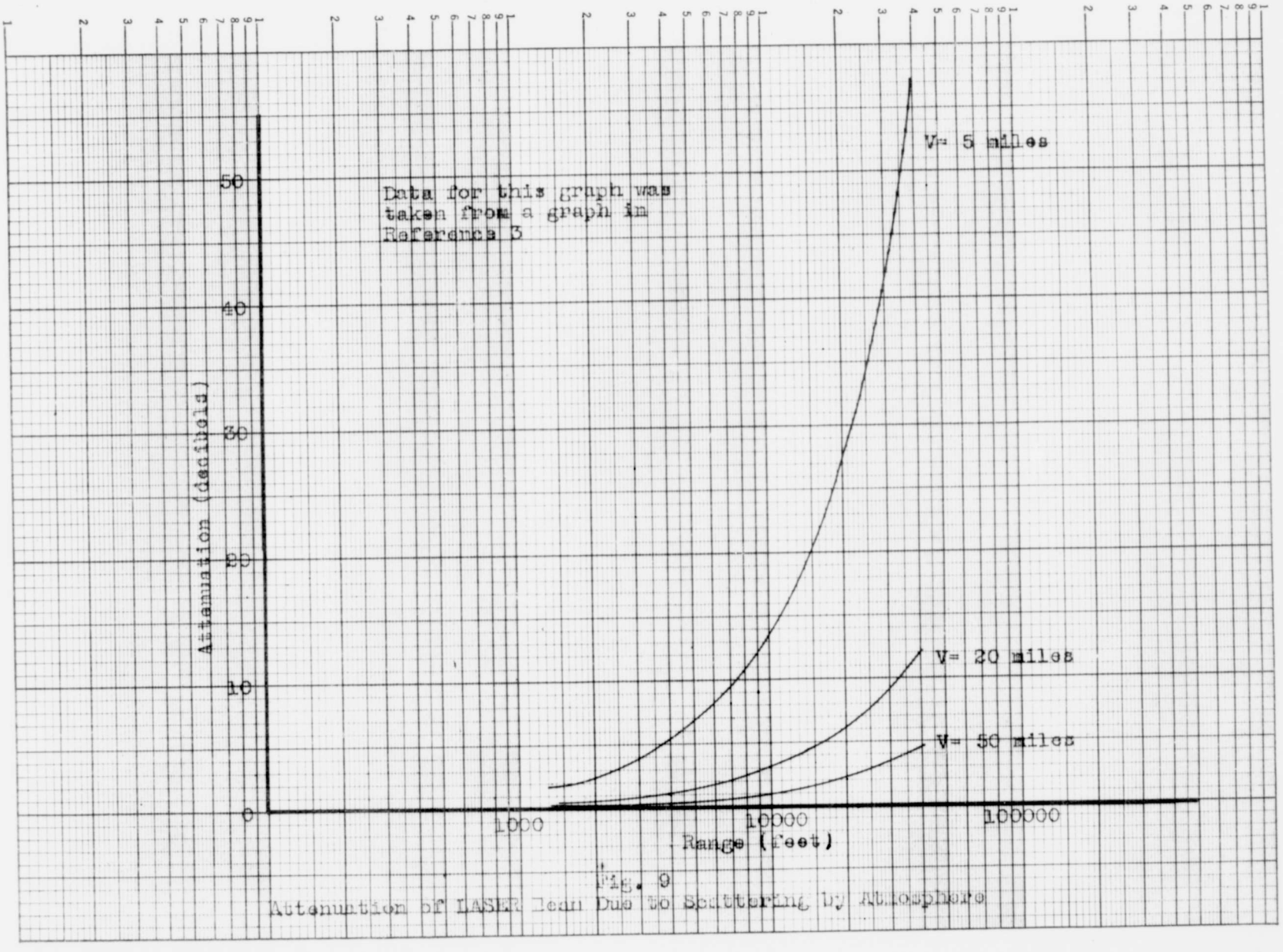

Fig. 9

Attenuation of LASER Beam Due to Scattering by Atmosphere

Fig. 10
Predicted Received Power With Atmospheric Attenuation

sphere. The assumption that these are the only significant sources of interference may be justified by considering the character and magnitude of the various possible sources.

The signal voltage of the anode of a photomultiplier when observed with a sufficiently wideband external circuit consists of discrete pulses having their origin in the emission of single electrons from the cathode. The large current amplification of the photomultiplier increases the magnitude of the current pulse to such a degree that the voltage pulse at the anode can be easily viewed on an ordinary oscilloscope. If the anode circuit consists of a resistor shunted by stray capacitance, which is the case in this system, the height of the average pulse will be

$$E = 1/c \; Ge \tag{5}$$

where c = stray capacitance

G = current multiplication of the photomultiplier (nominally 9.35×10^6 for the 7265)

e = electronic charge

The above expression is the initial response to a current impulse of a parallel RC circuit. The current output pulse of the 7265 is approximately 10^{-9} second in duration, and so closely approximates an impulse in this case.

The output capacitance of the 7265 is approximately 10 μμf and there is perhaps an additional 10 μμf stray capacitance in the

circuit. Then E = 0.075 volt. Thus, individual pulses due to single electrons are of considerable amplitude. A second case more representative of the actual situation in the system is where the extraneous light input to the photomultiplier is sufficiently great that the circuit cannot resolve individual pulses. If the number of pulses per second is 20 $\overline{\Delta f}$ or more (Ref 6), a modified shot noise formula

$$i^2_{r.m.s.} = 2 e G i \overline{\Delta f} \qquad (6)$$

may be used to find the root-mean-square fluctuation current at the anode, where $\overline{\Delta f}$ is the bandwidth of the circuit, i is the average anode current and the product e G is the electronic charge times the current multiplication of the multiplier. If $\overline{\Delta f}$ is 5 megacycles and the minimum 20 $\overline{\Delta f}$ pulses per second is assumed as an example, the $i_{r.m.s.} = 4.7 \times 10^{-5}$ amp, and if the anode load resistor is 100 ohms the root-mean-square fluctuation of the output voltage is 0.0047 volt. The thermal noise voltage of the load resistor would be far less than this and is therefore neglected. It is also assumed that the noise contribution of the preamplifier and oscilloscope amplifiers are negligible in comparison with this input noise. In the case of the low level noise where the result is discrete pulses or spikes, the criterion suggested by one investigator (Ref 4) regarding required signal-to-noise ratio for reliable signal detection is that the probability of more than a given number of noise pulses occuring

in one integration period of the circuit should be small since coincident pulses would form larger pulses that may be mistaken for the signal. The number of coincident noise pulses that would be designated would depend on the designer's criterion regarding the minimum detectable signal amplitude in the absence of noise. In the present system, as will be seen, the low noise level case will not be significant because the level of interference caused by back-scatter of the LASER beam by the atmosphere and by sunlight is well above the point where individual pulses are resolved. Following the suggestion of Smith and Stitch (Ref 8) the root-mean-square fluctuation of the anode voltage of the multiplier, as determined by the formula previously shown, will be taken as the noise level in determining the signal-to-noise-ratio.

The Dark Current. The dark current of a photomultiplier is the residual anode current which flows in the complete absence of light falling on the cathode. The maximum dark current of the 7265 at 25^{o} C according to the manufacturer, is approximately 8×10^{-7} ampere which is equivalent to 6.7×10^{-12} watts at 6943 Å falling on the cathode. As will be seen, this value of equivalent noise is negligible in comparison with the two remaining sources.

Sunlight Interference. Sunlight interference results from light being reflected from the target into the receiver and also from being scattered by the atmosphere into the receiver. Reference 8 provides

expressions for calculating the magnitude of the received power as a function of target range. Derivations of these expressions are given in Appendices B and C. Both assume a cloudless day and a uniform atmosphere. The sun power reflected from the target is given by

$$P = \frac{\pi B_0 e^{-bR} D^2 n_r H_S \omega^2 \rho \cos \phi}{16} \qquad (7)$$

where D, n_r, ω are given for equation (1) and

B_0 = width of the optical filter in Angstroms (nominally 10 $\mathring{A}$ in this system)

ϕ = angle between a perpendicular to the target and the direction of the sun

b = attenuation constant of the atmosphere

H_S = spectral irradiance of the sun at the target in watts per unit area per $\mathring{A}$ (0.01255 watt / $ft^2 \cdot \mathring{A}$) at 6943 $\mathring{A}$

In Appendix D, b is shown to be equal to 3.92 / V, V being the meteorological visibility, as a part of the derivation of the expression for LASER power backscattered by the atmosphere. The equation is shown plotted in Figure 11 for a representative set of conditions. As would be expected the power from the target decreases with distance to the target due to atmospheric attenuation.

The sun power scattered from the atmosphere and received by the system is given by: (Derivation in Appendix C)

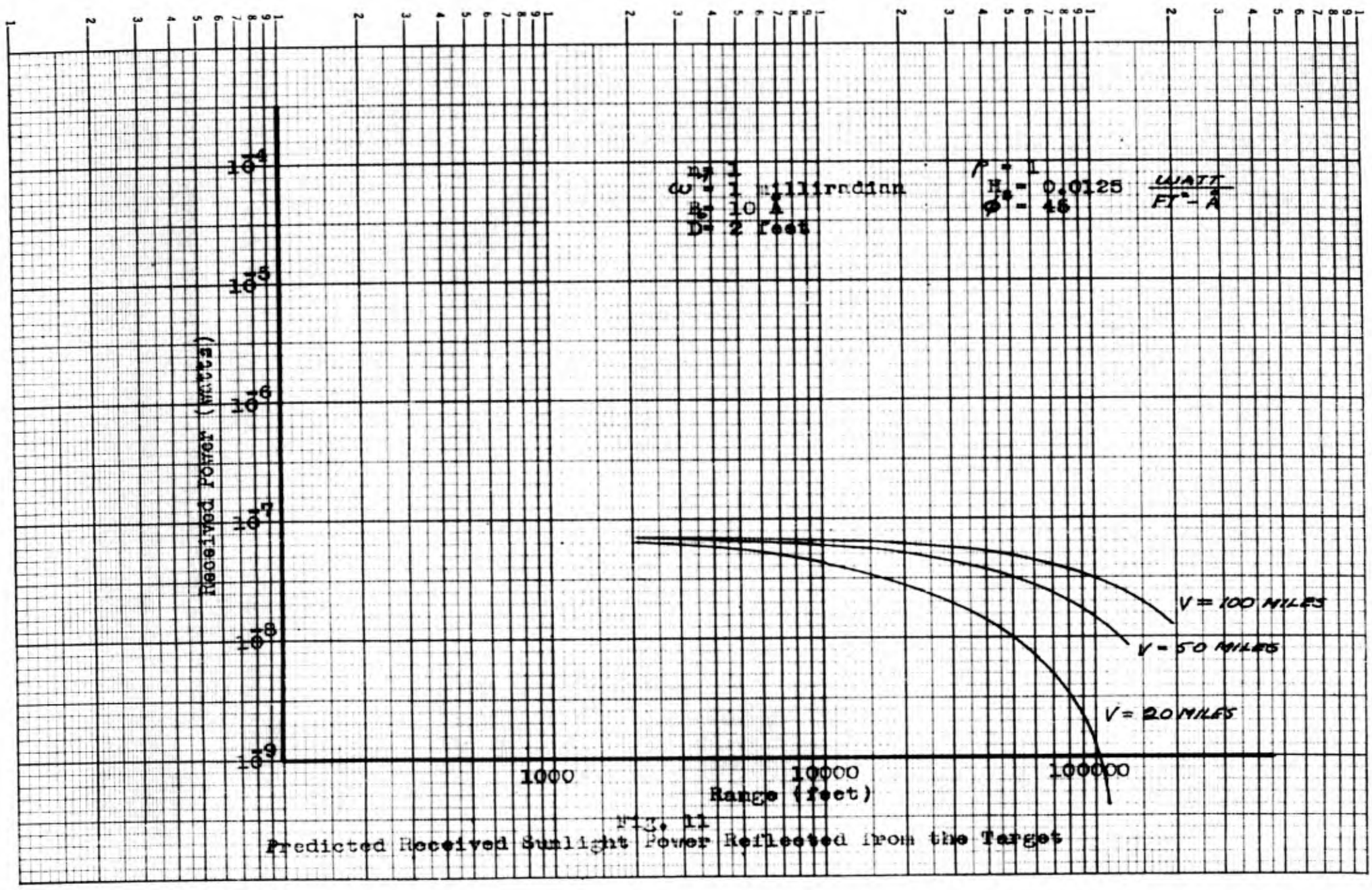

Fig. 11

Predicted Received Sunlight Power Reflected from the Target

$$P = \frac{\pi}{64} \; n_r \, D^2 \, B_o \, \omega^2 \, H_s \, (1 - e^{-br}) \qquad (8)$$

This expression is shown plotted in Figure 12 for the same conditions for which Figure 11 was plotted. In this case it is evident that the power scattered into the receiver increases with distance to the target since each element of the atmosphere along the path from the receiver to the target contributes to the power received. To obtain the total effect of the sun one must add the contributions from the target and atmosphere.

Backscattering of the LASER Beam. The LASER beam is scattered by the same mechanism that scatters the sunlight into the receiver. As will be seen backscattering is a serious limitation of a system such as this which uses a LASER with an extended output burst. The difficulty arises from the fact that the LASER continues to transmit pulses during the time that the received signal is being detected. As an example consider a target at a distance of 13,000 feet for which the ranging delay should be 26.4 microseconds. The LASER output burst lasts about 500 microseconds. The return signal is, then, being received while the transmitter is still emitting pulses. This transmitted energy is backscattered by the atmosphere and interferes with the signal from the target. A derivation is given in Appendix D of the following expression for the backscattered power as a function of range:

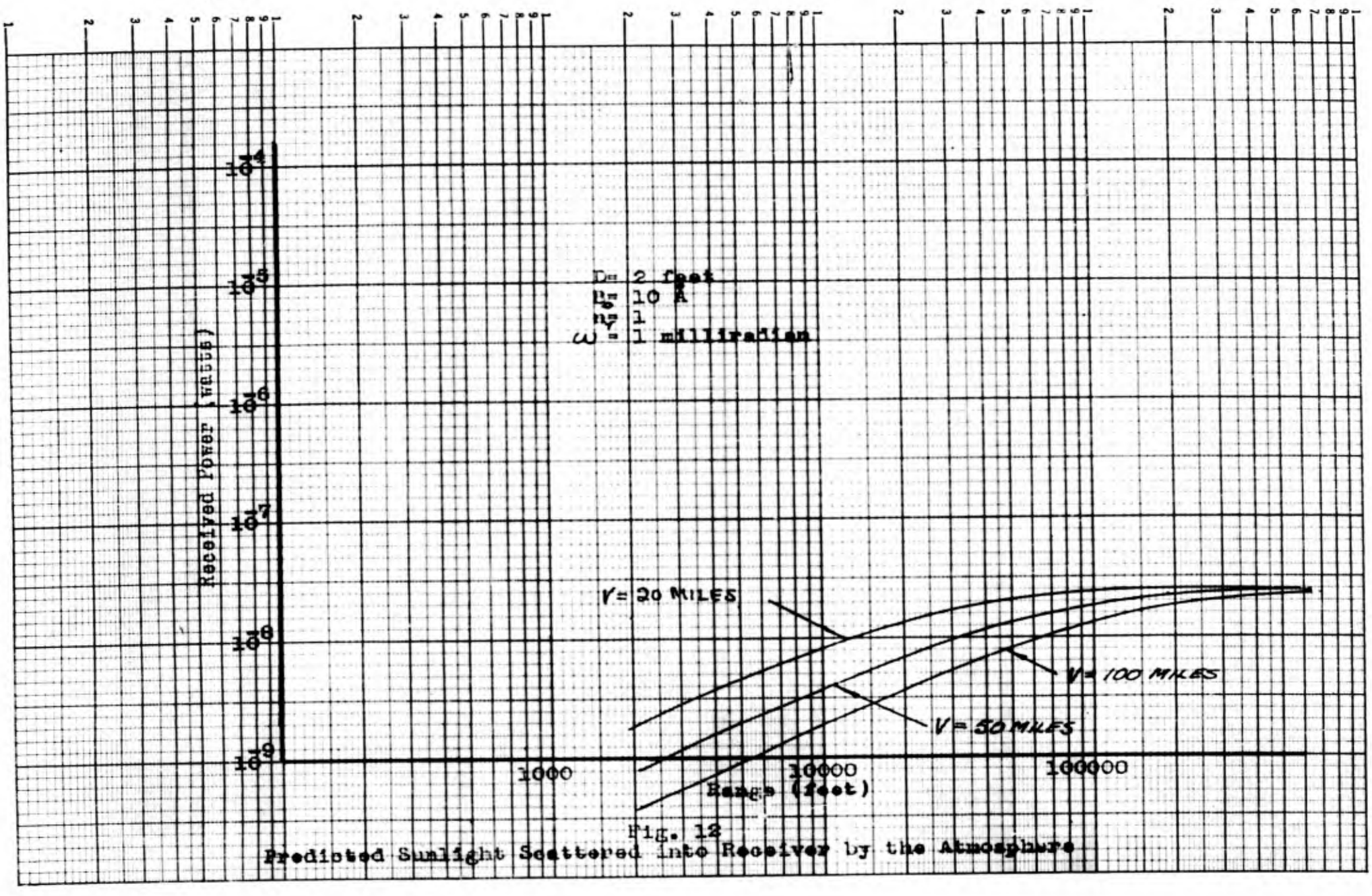

Fig. 12

Predicted Sunlight Scattered into Receiver by the Atmosphere

$$P = \pi B D^2 P_t \left(-2b E_i(-2br) - \frac{1}{r} e^{-2br} \right)_{R_0}^{R_T} \qquad (9)$$

where R_T and R_0 are limits of integration and

$$E_i(-x) = -\int_x^{\infty} \frac{e^{-t}}{t}\, dt$$ (may be evaluated by use of Reference 2)

$B = b/8\pi$

P_t = average transmitted power

R_t = range of target

R_0 = range of intersection of transmitting and receiving cones

In this equation it is assumed that the transmitter and receiver are separated by some distance such that scattering of LASER energy into the receiver field of view does not take place for a distance R_0 in front of the system. At R_0 the transmitted beam and receiving field of view are assumed to intersect completely. The intersection will not in reality, of course, take place at a point but will occur gradually over some distance. For purposes of

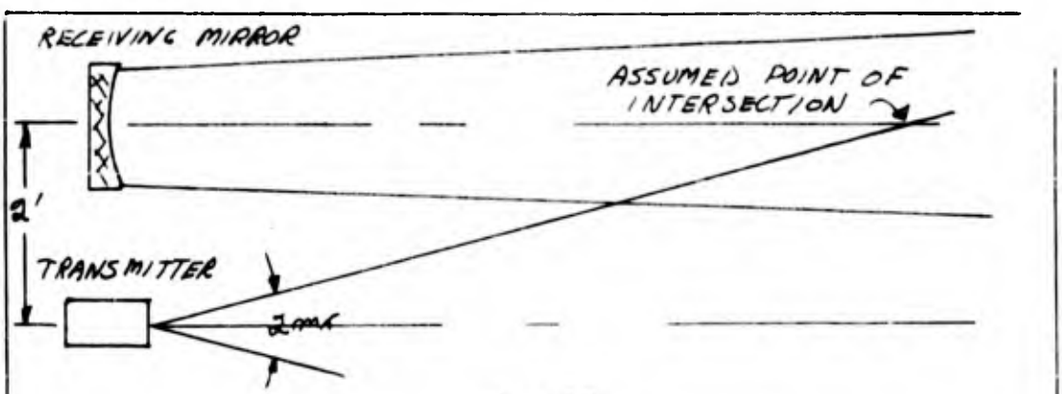

Fig. 13
Geometry of Intersection of Receiving and Transmitting Cones

comparison, the point of intersection was defined as the point where the 2 milliradian transmitting beam intersects the axis of the receiving mirror. This is shown in Figure 13. Since the separation of the axes of the transmitter and receiver is two feet, the point of intersection is 2000 feet in front of the system. With this definition of intersection point, the two cones are approximately halfway overlapping at R_0. Figure 14 is a plot of Equation (9) for R_0 = 2000' and 4000' and for different values of the visibility. The assumption of a distinct cone intersection point explains the rapid buildup of the curves at 2000 and 4000 feet. It is seen that the final amplitude at large ranges is less for the larger R_0. This results from the fact that the closer-in elements of the atmosphere contribute more backscatter than the distant ones.

Signal-to-Noise-Ratio

The signal-to-noise-ratio was predicted by combining the effects of background sunlight and backscattering of the LASER beam and comparing the attenuated signal return to this combination. Dark current was neglected in comparison with the other two sources. The combination of the two significant sources was done by addition of the power levels as a function of target range. The signal-to-noise-ratio is arbitrarily defined in two ways. First it is defined as the ratio of peak signal power to total noise power. This is done primarily as a matter of interest and so that comparisons of

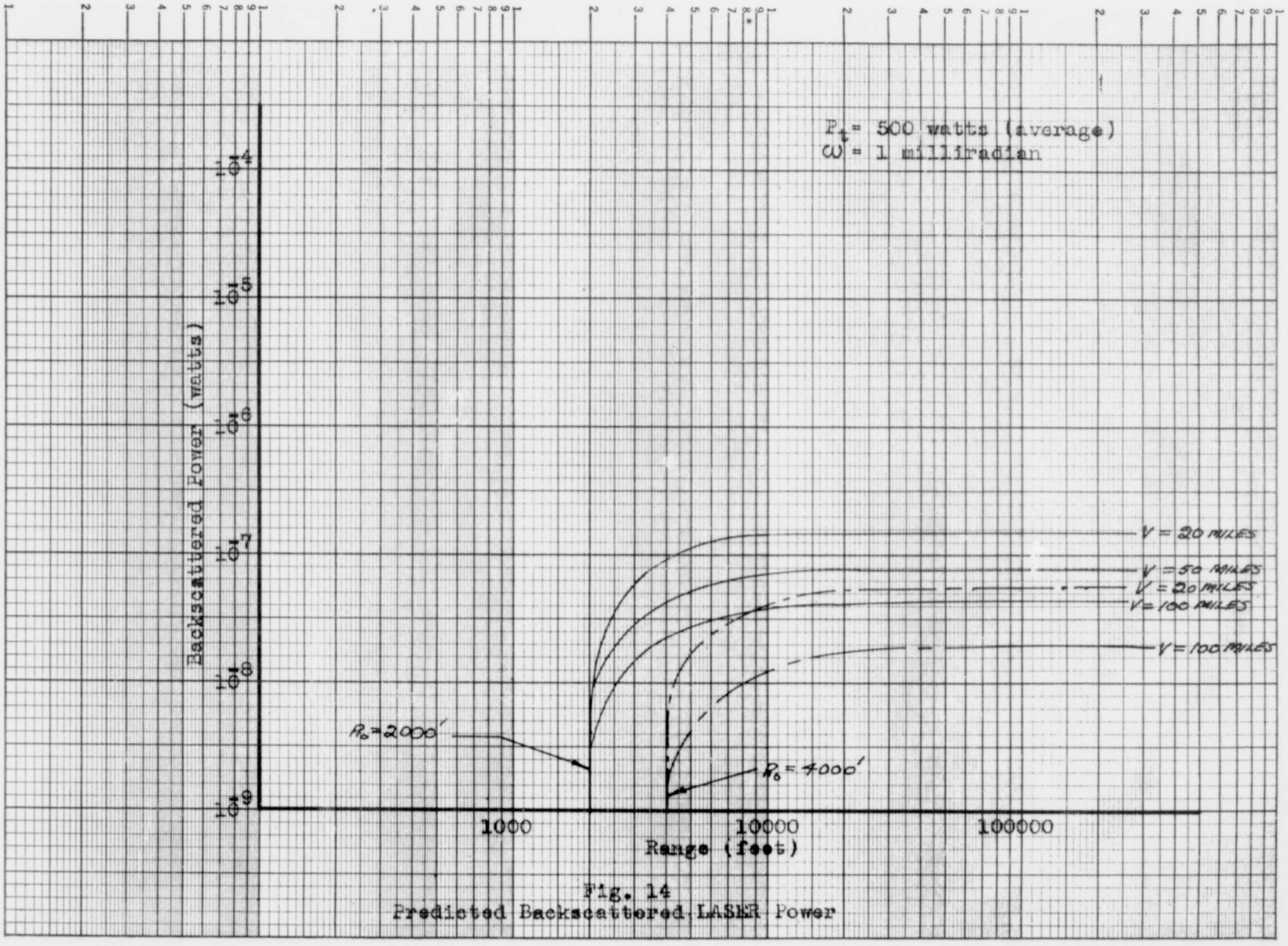

Fig. 14
Predicted Backscattered LASER Power

the signal and noise sources on a purely power basis can be made directly. As has been stated before, Smith and Stitch suggest that for high noise levels the degree of interference with the signal of a given amount of noise power is proportional to the root-mean-square fluctuation of the receiver output due to the noise input. The modified shot noise formula used previously is

$$i_{r.m.s.} = (2\,e\,G\,i_{av.}\,\overline{\Delta f}\,)^{1/2} \tag{10}$$

where $i_{av.}$ = average photomultiplier anode current. Through the definition of the sensitivity of the photomultiplier $i_{av.} = p_{av.}\,S_p$ and $i_{r.m.s.} = p_{r.m.s.}\,S_p$; S_p being the sensitivity. The p's are equivalent light input powers required to cause the currents $i_{av.}$ and $i_{r.m.s.}$ Therefore, upon substitution,

$$p_{r.m.s.} = \left(\frac{2\,e\,p_{av.}\,\overline{\Delta f}\,G}{S_p}\right)^{1/2}$$

is the noise level to which signal was compared to obtain signal-to-noise-ratio as a second and more useful definition. Figures 15 and 16 are plots of the predicted signal-to-noise-ratio versus range for a visibility of 20 miles and R_o = 2000 feet.

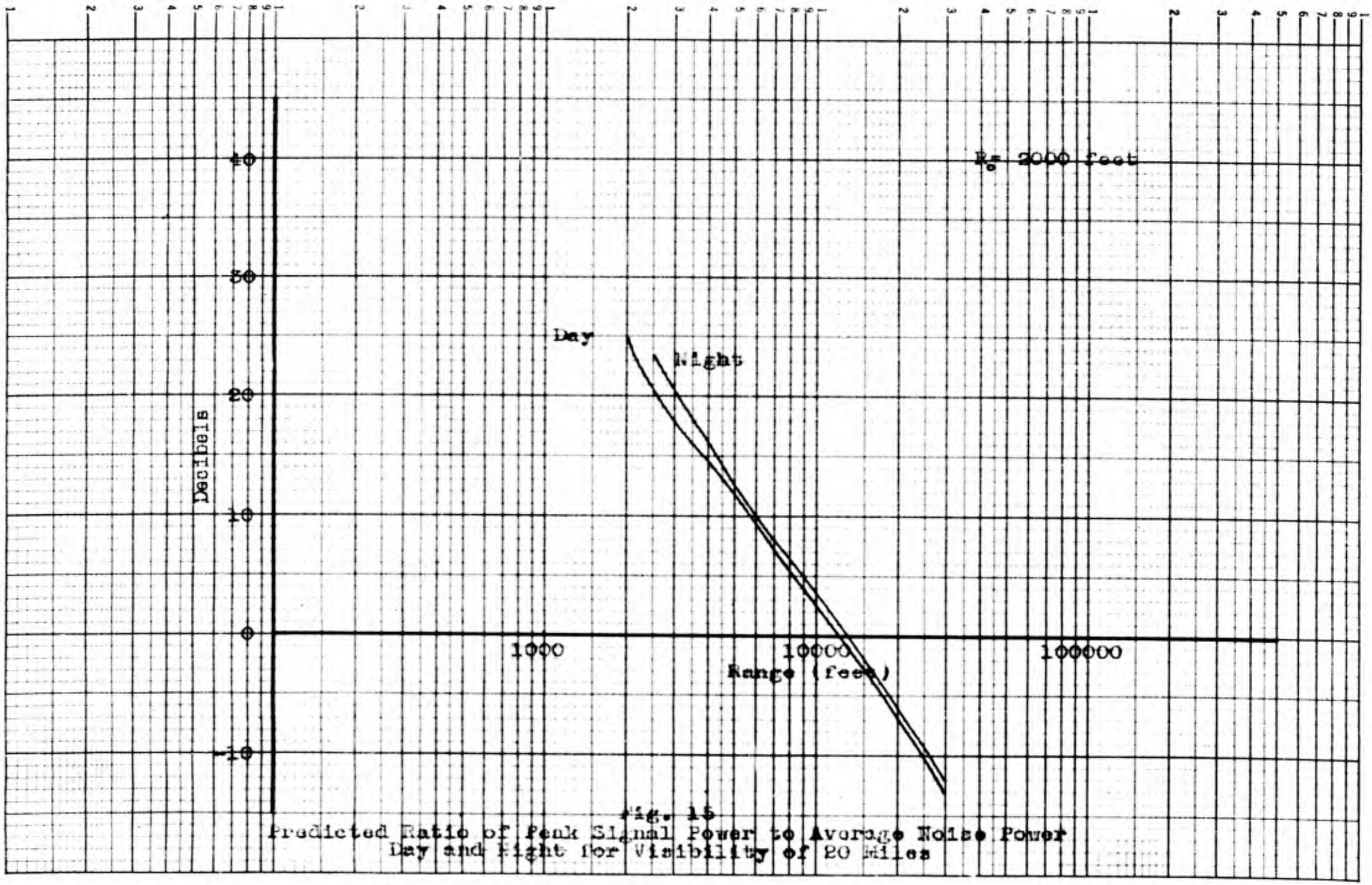

Fig. 15
Predicted Ratio of Peak Signal Power to Average Noise Power
Day and Night for Visibility of 20 Miles

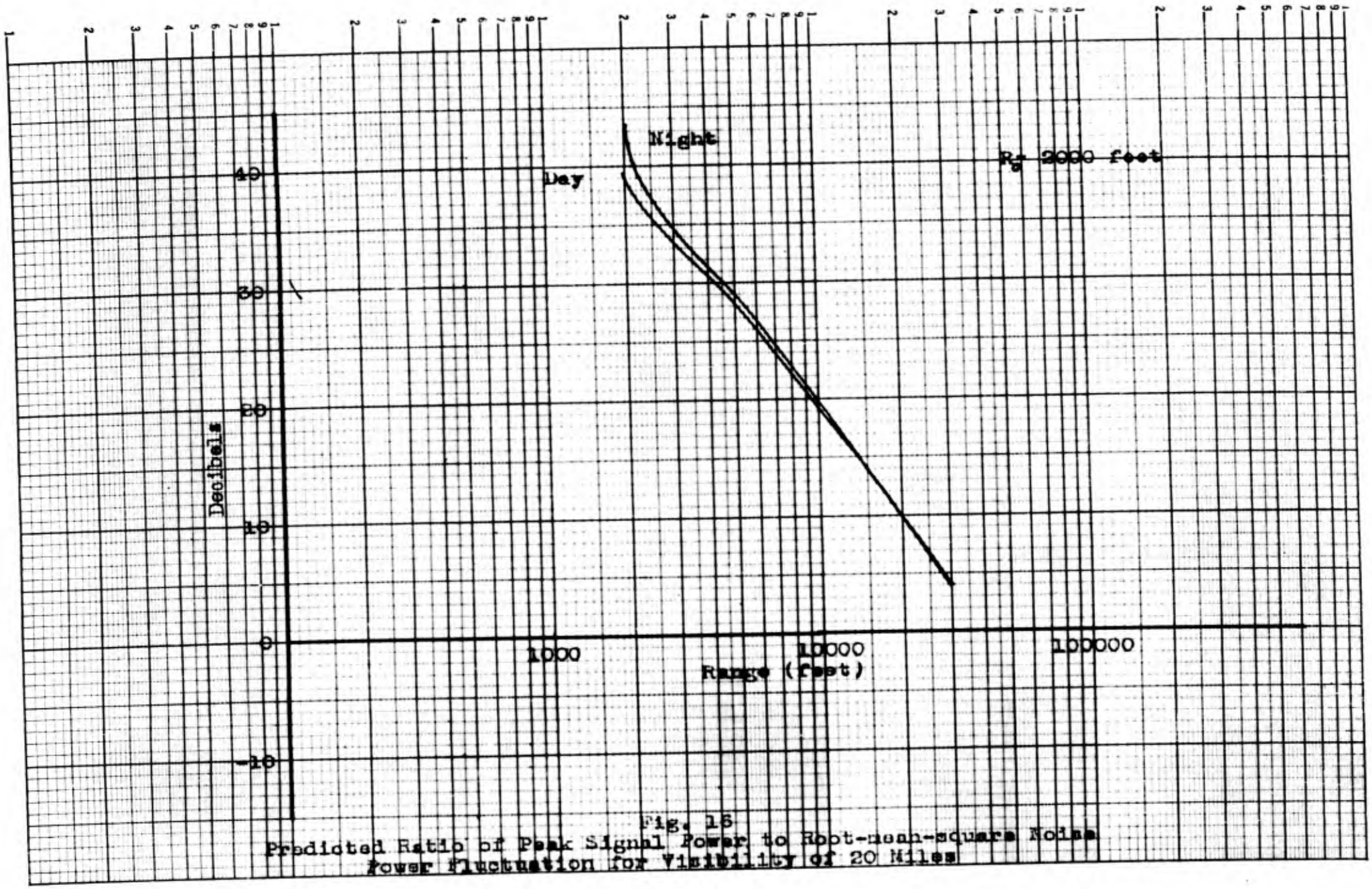

Fig. 16
Predicted Ratio of Peak Signal Power to Root-mean-square Noise Power Fluctuation for Visibility of 20 Miles

IV. Experimental Performance

Essentially, the experimental work had the objectives of (1) demonstrating that the system did obtain signals back from targets and (2) determining the signal-to-noise-ratio versus range. Four targets were chosen for the experiments that were readily visible from the test site and which stood well above the horizon. These targets and their distances are:

1. small water tank in front of Building 126 - 2300 feet
2. water tank along side of the Hilltop Theater - 4000 feet
3. water tank at Kemp and Smithville Roads - 13000 feet
4. water tank at corner of West Fairview Avenue and Ravenwood Avenue in Dayton - 32000 feet.

These targets were used throughout the experiment to demonstrate ranging, to obtain signal strength data, sunlight from target data and to perform focusing and alignment of the equipment.

Because of the one-shot nature of the LASER, and therefore of the system, almost all recorded data was derived from Polaroid photographs of single sweep oscilloscope traces. Two separate Tektronic 545 oscilloscopes were used to record the receiver output and the output of the trigger pickup unit simultaneously. The second oscilloscope was triggered by the sweep gate signal of the first, resulting in good synchronization of the two sweeps. It was possible to trigger the sweep of the master oscilloscope in two ways. The

first was to use the initial LASER output pulse. This resulted in a target return which showed the delay time quite graphically without reference to the transmitted waveform. An alternate method was to trigger the oscilloscopes from a trigger pulse provided by the LASER power supply. This pulse is coincident with the ionizing pulse for the flash tubes of the LASER. Since LASER output does not commence for roughly 250 microseconds after this time the sweep delay feature of the oscilloscopes was used to delay the sweep until LASER output had proceeded. This method has the advantage that the LASER can be allowed to develop full output before the sweep is begun and a more representative received power measurement can be made. Examples of returns from targets using the two modes of operation are presented in a later section.

A considerable amount of effort was spent on focusing the collimator and aligning the transmitting and receiving axes. Focusing was done by pointing the system at the Building 126 tank at night and observing the LASER flash as seen on the tank through the spotting telescope. The position of the negative lens in the collimator is adjustable and so was adjusted until the smallest spot of light was obtained. The final result agreed well with predicted beamwidth, the spot size being from about two to four feet in diameter, depending on LASER output power, at a distance of 2300 feet. Bore-sighting was done by firing the transmitter at the

Building 126 tank at night and aligning the spotting telescope to point at the same spot allowing for the slight parallax. At the next daytime opportunity the system was pointed at one of the more distant targets using the spotting scope. The photomultiplier head was then adjusted to place the opening of one of the small field stops on the target image. This procedure was repeated several times because the alignment seemed to shift unpredictably. Finally, it was discovered that the collimator mounting was responsible. The addition of stiffening members seemed to correct the difficulty.

As was seen in Chapter III, the meteorological visibility is one of the important variables effecting the performance of the system. Unfortunately, no accurate means of determining the visibility was available for the experiments. Furthermore, the visibility in one direction could be considerably different than in another. For example, the visibility in the direction of Dayton was almost certainly less than in other directions because of city smoke. The values of visibility given in the results which follow are estimates made in the following way. It was observed that on typical hot humid days for which a standard estimate of 20 miles visibility was made, the contrast of trees in Dayton against the western horizon as viewed from the test location on Wright-Patterson AFB at a distance of about 8 miles, was approximately minus one-fourth. This is equivalent to stating that the luminance of the intervening

atmosphere made the trees look three-fourths as bright as the background sky. The contrast of an object against the horizon as viewed from a distance R is (Ref 4:70)

$$Cr = C_0 e^{-\sigma R} \tag{12}$$

where C_0 is the actual contrast of the object against the sky when viewed at close range and σ is a constant depending on the visibility. The actual contrast of trees against the sky is close to maximum which is -1. If a value of $Cr = -1/4$, $C_0 = -1$ is inserted into (12), σ may be obtained. The same formula is then used to calculate R for which $Cr = -0.02$ which is the definition of meterological visibility. Doing so, one obtains V = 22.7 miles. This was rounded off to 20 miles for convenience since the accuracy of the estimate of contrast does not justify more than one significant figure. The estimate of 50 miles which was made for part of the data was for an exceptionally clear day just after a cool dry air mass had moved into the area. The value of 50 miles was given to indicate that the visibility was decidedly better than for the 20 miles case but has little numerical significance. Examination of the theoretical predictions shows, however, that the backscatter changes only 2.5 db or less when V changes from 50 to 100 miles and for the range being considered the attenuation changes even less. Therefore, if the results are not highly accurate they should at least be indicative.

Throughout the experiment a constant source of uncertainty was the power output of the LASER. One reason for this was inconsistent or erratic firing of the four Xenon flash tubes. As the tubes aged, higher and higher voltages were required to make them fire with any degree of reliability with resultant higher energy output. This was partly compensated by the natural behavior of the LASER, i.e., the power output on peaks of the LASER does not appear to change in direct proportion to the energy output but rather the number of pulses per unit time also changes. In other words, there seems to be some tendency for the pulses to maintain their amplitude with changes of total energy output. This observation is backed up qualitatively by noting the relatively constant amplitude on the average of the transmitted signal waveforms presented later in this section.

Demonstration of Ranging

Signal returns were obtained from three of the four targets. No attempt was made to obtain a return from the Dayton Tank because of time limitations. Figure 17 shows examples of returns from the Building 126 tank and the Hilltop Theater tank. With reference to the photograph pertaining to the 126 tank, the two upper traces show the waveform of the return signal for two separate shots. The sweeps in all cases in the photographs presented start on the right hand side of the scale. In these particular cases, the

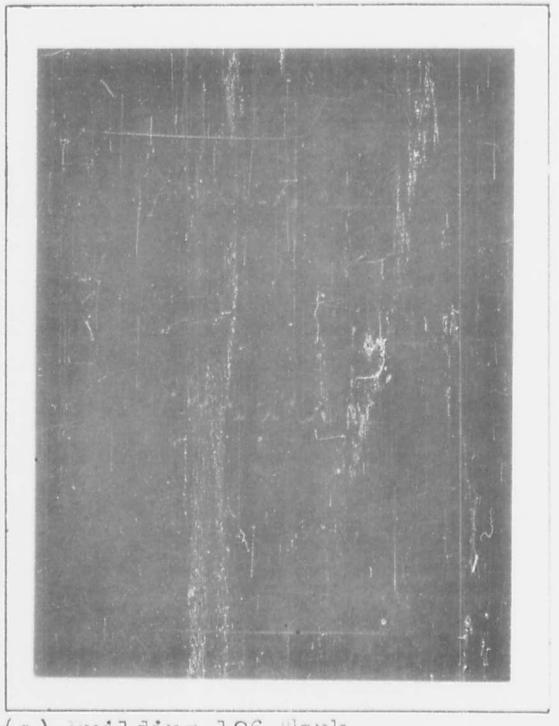

(a) Building 126 Tank
Top trace- pointed at tank
Bottom trace- slightly off tank
Sweep speed 2μs/div.

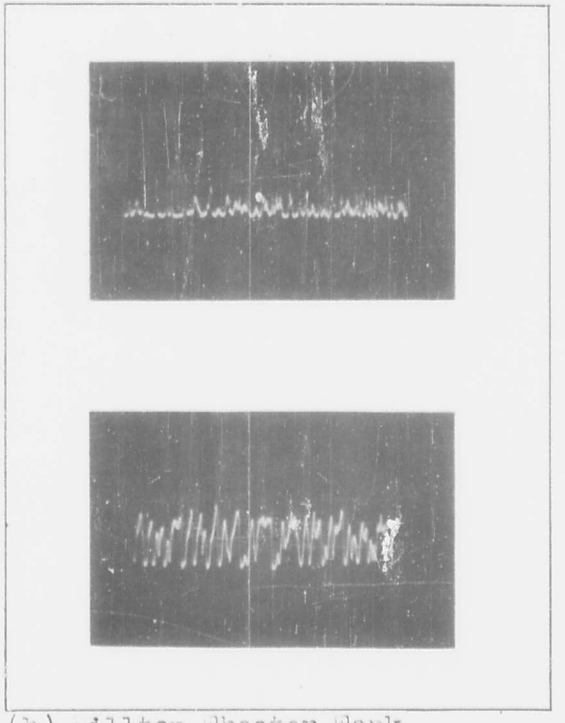

(b) Hilltop Theater Tank
Top trace- received signal
Bottom trace- transmitted signal
Sweep speed- 10μs/div.

Fig. 17
Examples of Return Signals from the Building 126 Tank and the Hilltop Theater Tank

oscilloscope sweep was triggered by the initial transmitted pulse as picked up by the trigger pickup unit. The sweep speed was 2 microseconds per centimeter. The time delay incurred by the signal is approximately the blank part of the trace on the right. It is only approximately so because the sweep was triggered somewhat erratically by the irregular LASER signal. This is seen by comparison of the two sweeps which show somewhat different results and illustrates one of the disadvantages of this mode of operation. The bottom trace was the result when the system was directed slightly away from the target into the adjacent sky and is evidence that the other traces do represent signals coming from the tank.

Figure 17b shows the transmitted and received waveforms for Hilltop tank. The sweep speed was 10 microseconds per centimeter. This is an illustration of operation employing the delayed sweep function of the oscilloscopes. The sweep began 500 microseconds after the ionization pulse for the LASER flash tubes and therefore, perhaps 200 microseconds after LASERing began. The top trace is the received waveform and the bottom trace is approximately the transmitted waveform. Unfortunately, the high frequency response of the trigger pickup unit is not as good as it should be for purposes of correlating with the received signal because the circuit was not originally designed with that in mind. It was designed for triggering the receiving oscilloscope sweep on the initial LASER pulse. This

lack of high frequency response if chiefly responsible for the difference in appearance of the two sweeps. However, the correlation is unmistakable after study of the pulses. There is an 8 microsecond time delay for this target. To aid in seeing this correlation, thirteen of the more prominent received pulses were chosen and the corresponding transmitted pulses were located. The horizontal coordinates of the pulses measured in microseconds from the left hand end of the scales are given below. It is apparent that

Coordinate of Received Pulse (μ sec. from left)	Coordinate of Transmitted Pulse (μ sec. from left)	Time Difference (μ sec.)
98	90	8
93	85	8
89	81	8
87	79	8
82	74	8
79	70	8
73	65	8
67	59	8
44	36	8
40	32	8
38	30	8
33	25	8
28	20	8

the time delay between the listed pulses is appropriate. The amplitude correlation is not as good as the time correlation, partly because of the relatively poor transient or frequency response noted previously.

Figure 18 shows the transmitted and received waveforms when the system was directed at the Smithville Road Tank and when the

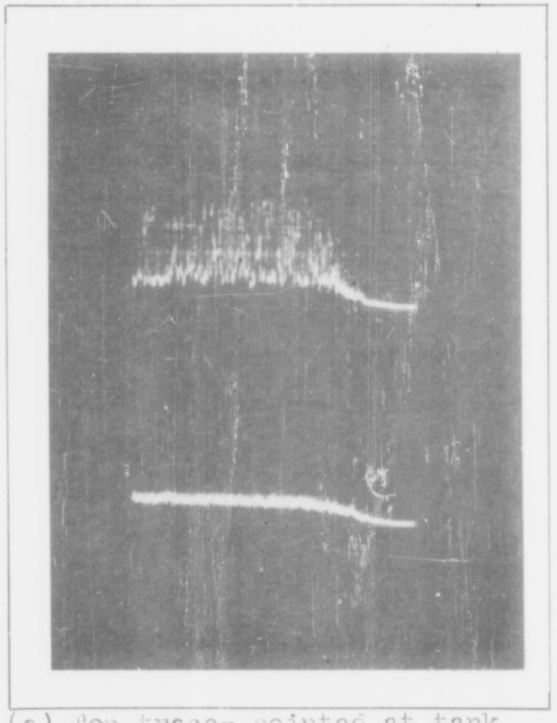

(a) Top trace- pointed at tank
Bottom trace-pointed slightly away from tank

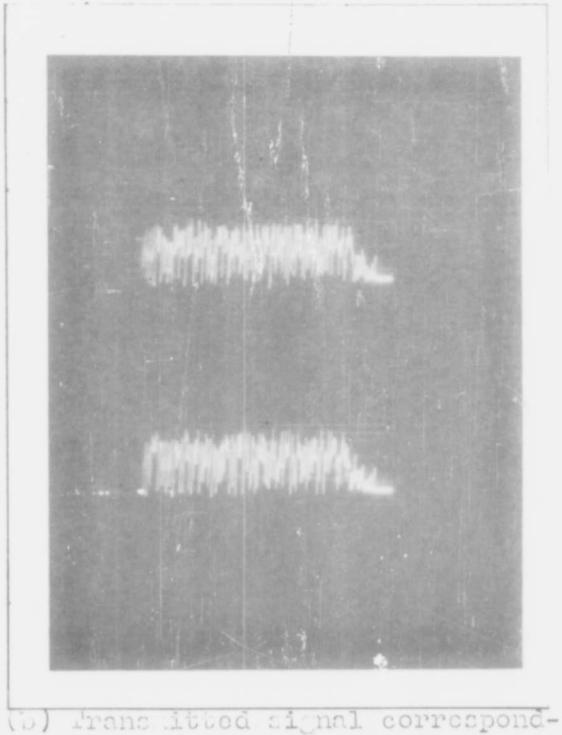

(b) Transmitted signal corresponding to received signals of (a)

Sweep speed 20 μsec./scale division

Fig. 18

Signal Returns from the Smithville Road Tank

system was directed slightly away from the tank. The (a) photograph is the received signals and (b) the transmitted signals. The sweep speed was 20 microseconds per centimeter so that a good part of the entire LASER burst can be seen. The delay should be 26.5 microseconds which it is seen to be approximately by observation of the general shift to the left of the received signal relative to the transmitted signal. The general rise of the baseline of the two received signal traces is due to backscatter from the atmosphere and will be discussed in a later section. Obviously, the echo signal is not seen in the bottom receiver trace since the system was pointed away from the target.

Numerous photgraphs of the type shown above were made but no purpose is served by discussing them all since the properties of the ones shown are representative.

Measurement of Background Sunlight

Measurements of the sunlight reflected from the target and scattered into the receiver by the atmosphere were made on a sunny day when the visibility was estimated at 20 miles. A sunny day was chosen since this is the brightest condition and because the theory of Chapter III was based on that assumption. Since the sunlight from the target and from the atmosphere are inseparable by the receiver, a measurement of their combined contributions was made on each of the four targets. This was done by pointing the receiver at the

targets in turn and reading the average photomultiplier anode voltage using the Tektronic 545 oscilloscope. At the high light levels involved the d-c component is large and is easily measured. A 50,000 ohm anode load resistor was used with the photomultiplier to help make the voltage large also. To represent a typical case it was attempted to make ϕ (see equation (7) on page 26), the angle between a perpendicular to the target and the direction of the sun roughly 45^{o} for all the targets. This required making the measurements on the Building 126 Tank and the Hilltop Tank in the afternoon and on the two other tanks in the morning. While making each of these measurements, a measurement was made looking slightly away from the targets. The results appear in Table I.

As a representative situation, theoretical curves for the combined sunlight from the target and sunlight scattered into the receiver were plotted for $\phi = 45^{o}$, $n_r = 1$, $\rho = 1$, and $\omega = 0.13$; the latter being used since that is the value of ω that was used in the experiment. This is the upper limit regarding n_r and ρ, but the curves may be shifted down by an appropriate number of decibels in cases where better estimates of those factors are available. Figure 19 shows the theoretical curves and actual receiver response for the four targets. These points were calculated from the data shown in Table I using the d-c anode voltage column only by means of the formula

Table I

Background Sunlight Data Summary

$B_o = 10$ Å; $\omega = 0.13$ mr; $\phi \doteq 45^o$; V $\doteq$ 20 miles

Target	Time (est)	7265 D.C. Anode Voltage (50 K Load)	R.M.S. Anode Voltage x 9 $R_{Lp} = 500$	$R_{Lp} = 100$
*Smithville Tank	1030	28	0.9	0.2
Sky Adjacent to Tank	1035	16	0.68	0.15
*Dayton Tank	1100	24	0.82	0.18
Sky Adjacent to Tank	1100	16	0.68	0.14
Dayton Tank	1445	24	0.83	0.18
Sky Adjacent to Tank	1450	30	0.92	0.20
*Bldg. 126 Tank (White Square)	1500	50	1.2	0.29
Sky Adjacent to Tank	1510	14	0.59	0.125
Bldg. 126 Tank	0955	12	0.6	0.13
Adjacent Sky	1000	40	1.2	0.27
*Hilltop Theater Tank (White Square)	1545	52	1.25	0.29
Adjacent Sky	1550	12	0.56	0.12

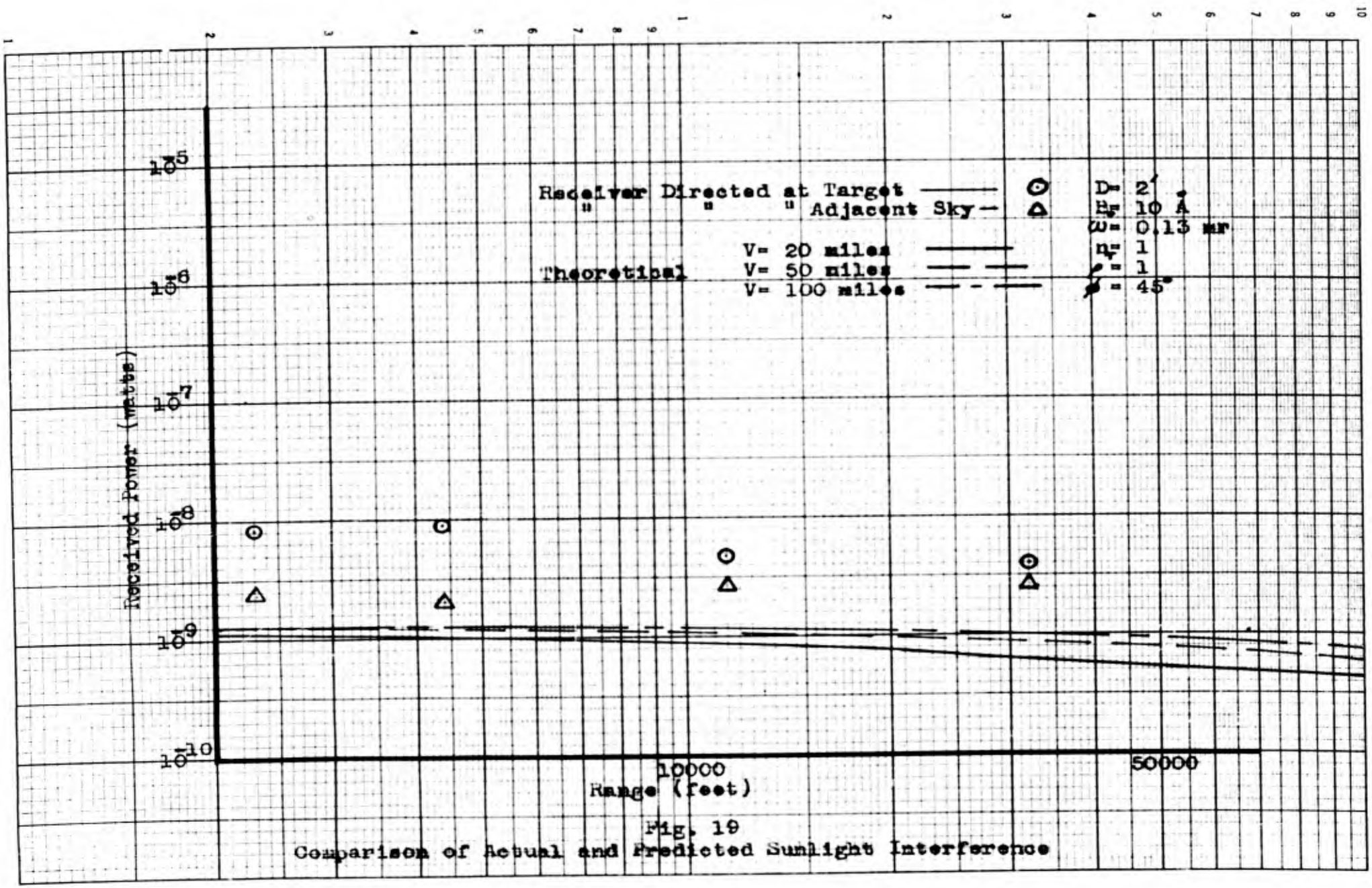

Fig. 19

Comparison of Actual and Predicted Sunlight Interference

$$P = \frac{V}{R_{Lp} S_p} \tag{13}$$

where P = power received

V = d-c voltage across 7265 anode resistor (50 K)

R_{Lp} = value of anode resistor

S_p = 7265 sensitivity, assumed to be 0.12 ampere /microwatt

The four entries used (See Asterisks) from the table were those corresponding to the morning hours for the Smithville Tank and Dayton Tank and the afternoon hours for the Building 126 Tank and Hilltop Theater Tank, in which cases $\phi \doteq 45^{o}$. The circled points of Figure 19 show the measured receiver response when the receiver was pointed at each of the targets. The reflectances of the two shorter range targets are in all likelihood greater than those of the other two targets since the former are quite white whereas the Smithville Tank is gray and the Dayton Tank is a light green. Color is, however, not necessarily a reliable index as may be seen in Reference 1, pages 6-42 where 26 common objects or surfaces of various colors are listed. In general, only blue and dark green objects drop below about 0.5 at 7000 $\mathring{A}$ whereas the majority are in the range 0.7 - 0.98. Therefore, it seems fairly safe to assume that reflectance will account for not more than a 2 decibel variation in the level. Other sources of error in the two measurements on the two more distant targets are shape of the targets and departure

of the target surfaces from ideal diffuse reflectors. In general, it can be seen that the trend of the circled points is downward with range as the theoretical curves predict. The triangular points are the receiver response with the receiver looking at the sky adjacent to the targets. Theoretically these points are at the same level and should be the limiting level of the circled points as range increases. An asymtotic level for the theoretical curves is shown by the arrow. It is apparent that the level of the measured points is about 8 decibels higher than the theoretical. This is attributed primarily to errors in assumptions regarding the effective B_0 of the optical filter and the sensitivity of the 7265. Furthermore, there is undoubtedly a considerable amount of light scattered from the receiving mirror into the photomultiplier due to surface imperfections and dust. With reference to Table I, the entries regarding the Dayton Tank in the afternoon and the Building 126 Tank in the morning are data for cases where the targets are backlighted. It can be seen that the brightnesses of the adjacent sky in these cases are considerably greater than in the cases considered before. This shows a weakness of the theoretical result which does not take into account the angle between the direction of the sun (See Appendix C) and the line of sight of the receiver in calculating the scattering into the receiver by the atmosphere. A check was made near noon of the same day the data of Table I was taken and values of 19 and 21 volts across the 50 K anode load

resistor were read for the eastern and western horizons respectively, indicating fairly equal brightness in this special case.

Backscatter from the Atmosphere. Backscattering of the LASER beam from the atmosphere was measured by directing the system slightly above the horizon at night and photographing the return signal trace. A series of shots were made for two rather widely different values of visibility. Figure 20 shows the six sets of transmitted and received waveforms for the case when V was estimated at 20 miles. All four available fields of view, except ω = 2 milliradians which caused receiver overloading, were used in order to determine if a discernable difference in the magnitude or character of the return signal could be detected for the different fields of view. On the basis of the theory of Chapter III, it would be expected that the beginning of the backscattered signal would occur at a later time for the smaller fields of view because the receiving and transmitting cones would begin to overlap at a greater distance from the equipment.

Examination of photograph set 108-109 reveals the typical character of the backscattered signal. As time progressed from right to left the transmitted power output commences with a fairly fast rise. The received signal rises more slowly because the signal is built up by contributions from greater and greater distances past the beam crossover point until it reaches a maximum and maintains it.

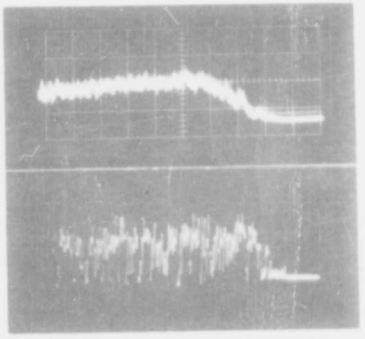

SET 108-109, $\omega = 0.9$
$R_{LP} = 100$, 5v/div

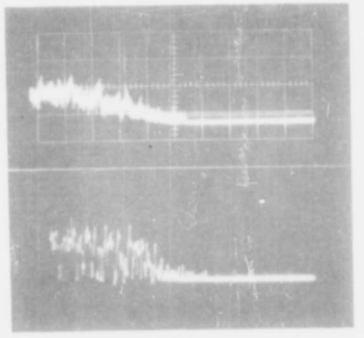

SET 110-111, $\omega = 0.5$
$R_{LP} = 500$, 5v/div

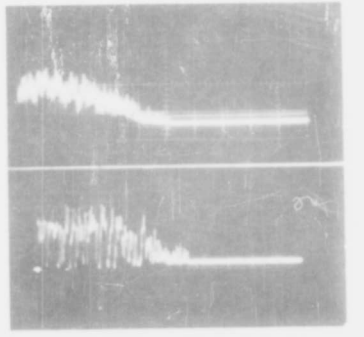

SET 112-113, $\omega = 0.5$
$R_{LP} = 500$, 5v/div

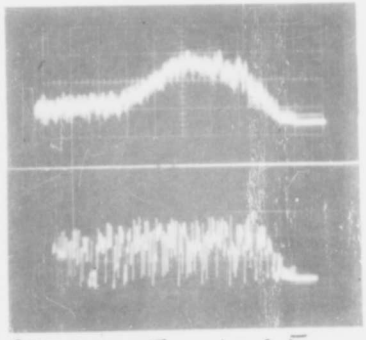

SET 114-115, $\omega = 0.5$
$R_{LP} = 500$, 5v/div

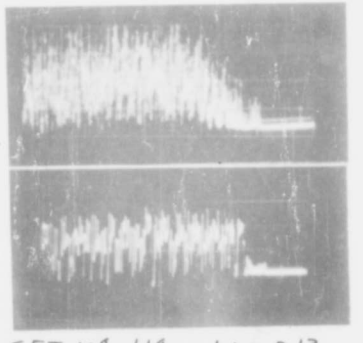

SET 118-119, $\omega = 0.13$
$R_{LP} = 1000$, 1v/div

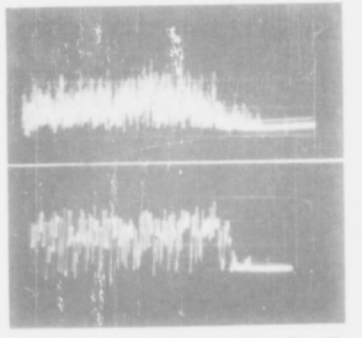

SET 120-121, $\omega = 0.13$
$R_{LP} = 1000$, 2v/div

Sweep speed 20usec./div.

Fig. 20

Photographs of the Signal Due to Backscattering of the LASER Beam and the Corresponding Transmitted Signals for a Visibility of 20 Miles

The most convincing argument that the signal is indeed from backscatter is that the receiver is unable to resolve the signal into distinct pulses. It has been demonstrated that the receiver resolves quite well the individual pulses of a return from a discrete target. In the case of backscatter the returning photons arrive at essentially random times. If the number per unit time is sufficiently great, the receiver is unable to resolve the individual pulses. The result is a fluctuation voltage superimposed on the instantaneous average value. The instantaneous average value of the trace may be observed to fall off as time increases past the peak level. This is due to insufficient low frequency response in the preamplifier which consequently will not allow a sustained d-c level to exist. The average level should be fairly constant during the less than 200 microsecond period shown. The other compelling argument that the signal obtained is backscatter is the shape of the build-up of the average value. The theory predicts a build-up with range (or time) as shown by the plots of the theoretical result in Figure 14. The theory assumes, however, that the transmitting and receiving cones intersect at a well defined distance in front of the system and that the power output from the transmitter is constant from t = 0. Figure 21 is a plot of the actual envelopes of the received signals with the amplitudes normalized to a field of view of 1 milliradian and a photomultiplier load resistance of R_{Lp} = 100 ohms. The data was obtained by sketching

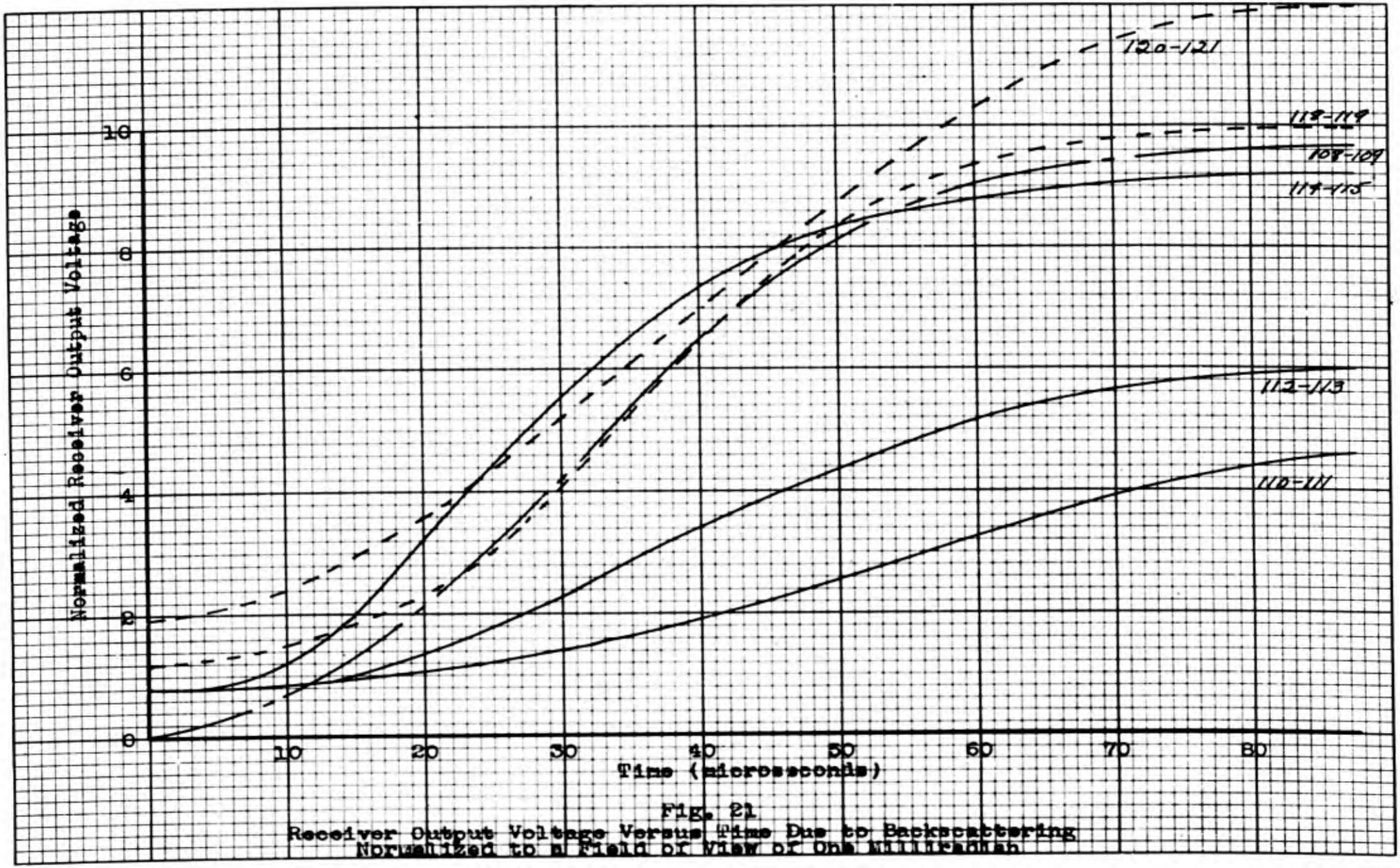

Fig. 21
Receiver Output Voltage Versus Time Due to Backscattering
Normalized to a Field of View of One Millisteradian

a smooth curve through the fluctuating portion of the traces and subsequently reading the amplitude versus time of this curve.

The normalization would ideally tend to make the final amplitudes of the curves equal. Reference to photographs 110 and 112 reveals that the LASER output had a slower onset than was the case for all the other shots. They also show qualitatively that the average power output of the LASER was probably less than for the other shots as indicated by the fact that the oscilloscope trace was able to reach the baseline level more often than for the others. This lower power output was probably due to misfiring one or more of the gas discharge tubes of the LASER. The slow onset of power and smaller average power for sets 112-113 and 110-111 are believed to be the reason for their deviation from the general level of sets 108-109, 118-110 and 114-115. The deviation of set 120-121 could easily be due to an error in determination of the average value of the amplitude because of the large fluctuation of the signal in this instance. This large fluctuation, incidentally, arises from the fact that the rate of returning photons is small enough to begin to allow the photomultiplier to resolve the individual anode current pulses. The shape of the received signal of set 114-115, i.e., the failure of the average value to remain at approximately a constant level is unexplained but is believed to be due to a circuit transient or perhaps a power line fluctuation because it was the only result of this

kind out of all the backscatter data. Figure 22 is a plot of the onset of the transmitted power envelopes normalized to the same final level. The data for these curves was obtained in the same manner as for the received signal but the results in this case are meant only to show the general shape of the power buildup. They show that the power onset was about the same for all sets but 112-113 and 110-111. It can further be seen qualitatively that the received signals of these two sets would conform to the other sets more closely if they were corrected for this slow onset of power. It was decided after the above considerations that the results of 108-109 were representative of the group. An average could have been taken but the general precision of the method of measurement did not seem to justify it. Figure 23 is a plot of set 108-109. Also plotted here are the results of a second set of backscatter data photographs which the visibility had been estimated at 50 miles. These were all made with ω = 0.9 milliradian since this aperture gives a high enough power return to result in a signal well integrated by the receiver and yet does not overload the receiver. This latter set of photographs are shown in Figure 24. It is seen that these are essentially uniform in response and so there is little doubt that they are representative. Also plotted in Figure 23 are the theoretical curves so that a comparison is convenient. First, it may be observed in Figure 23 that the buildup is slower for the actual curves than for the theoretical

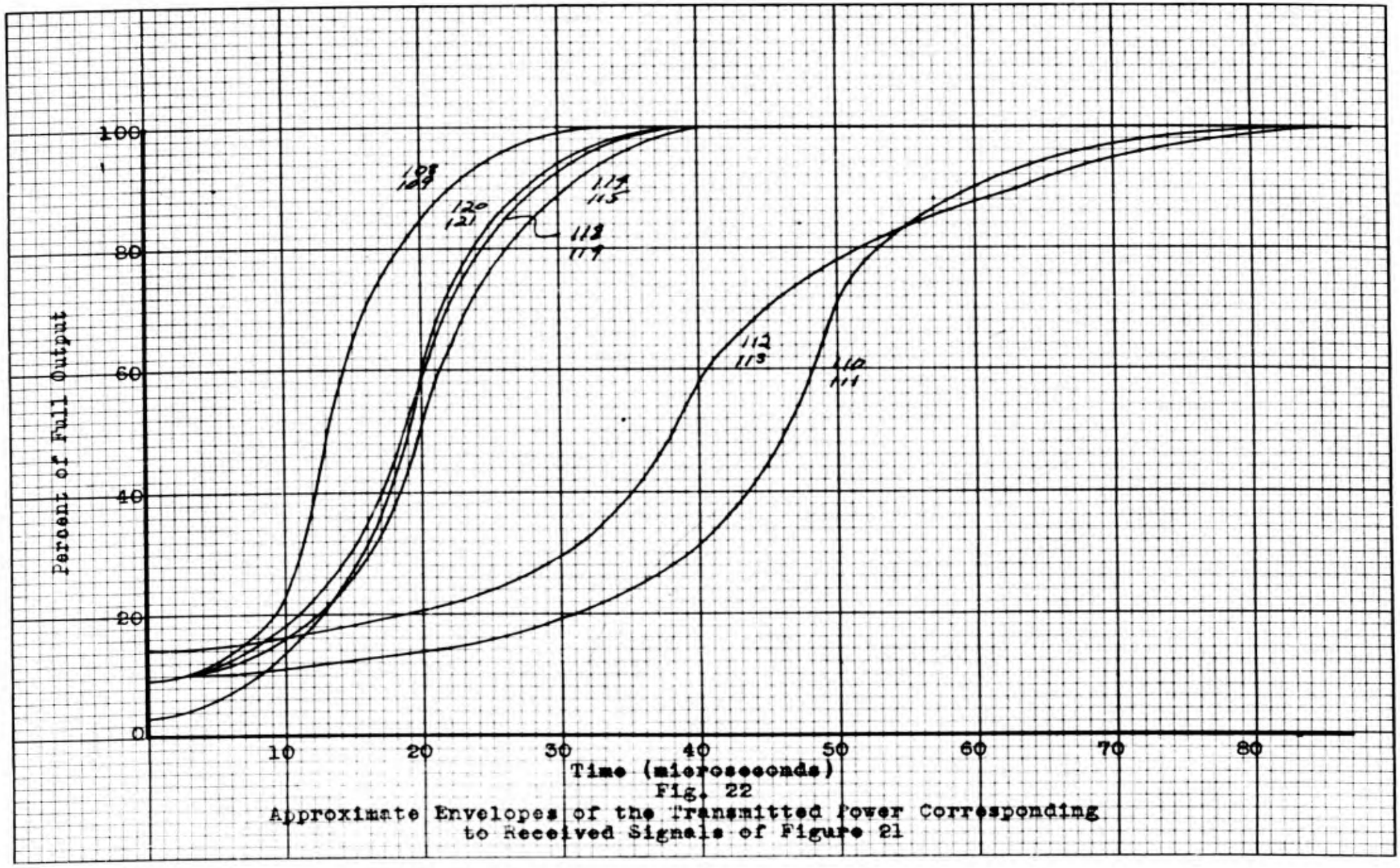

Fig. 22

Approximate Envelopes of the Transmitted Power Corresponding to Received Signals of Figure 21

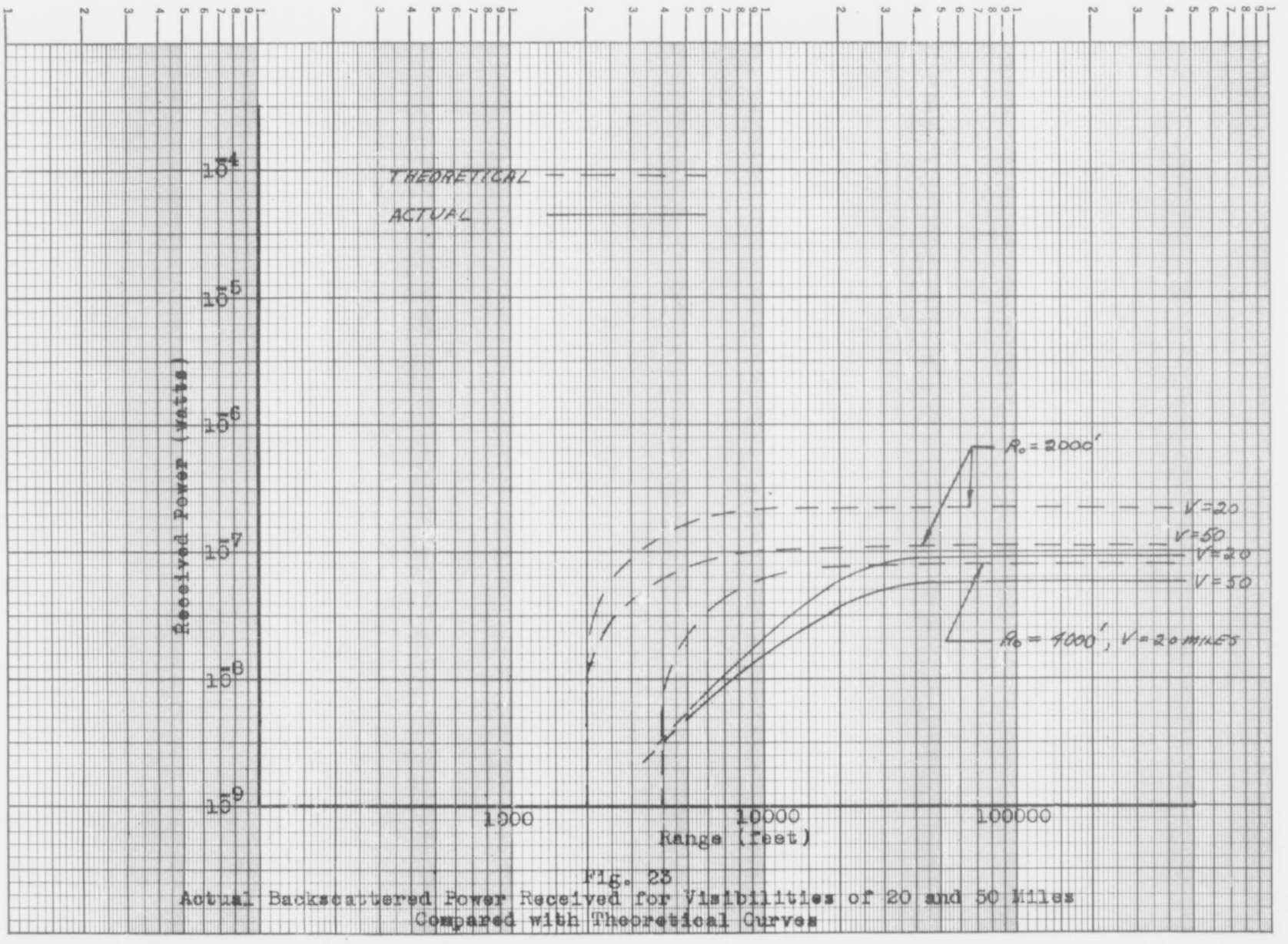

Fig. 23
Actual Backscattered Power Received for Visibilities of 20 and 50 Miles
Compared with Theoretical Curves

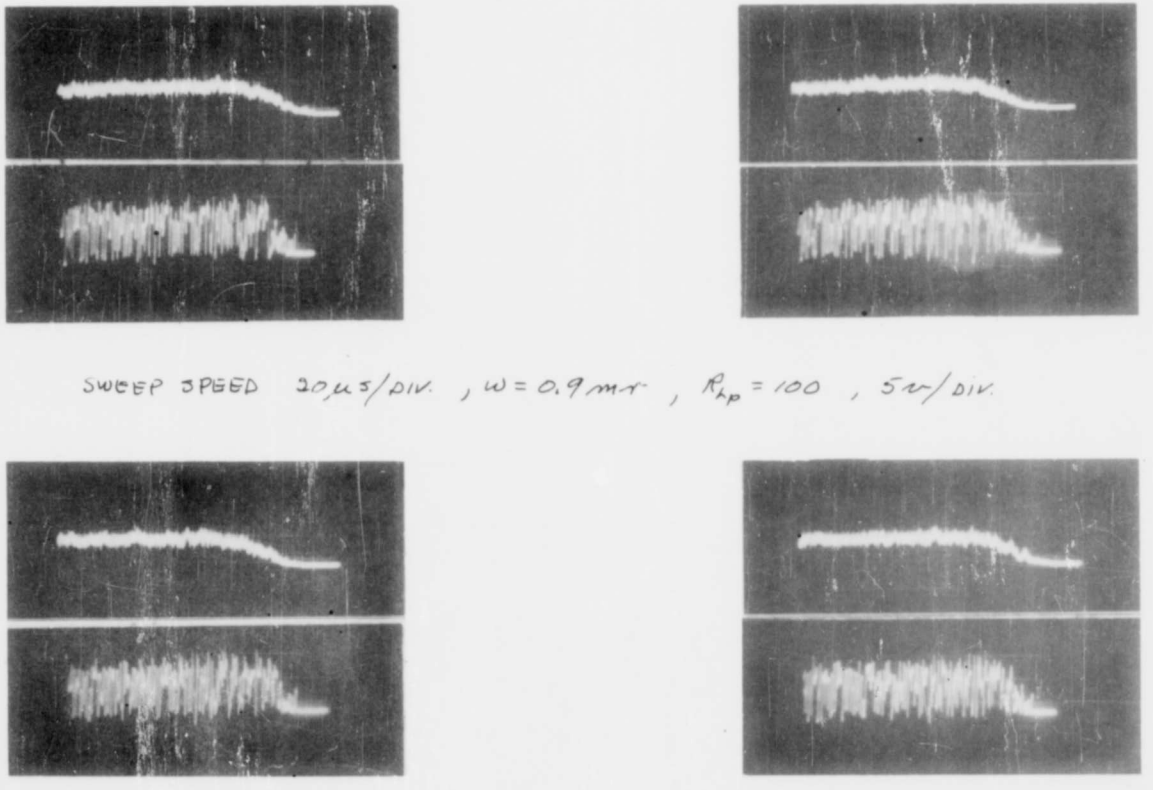

Fig. 24
Backscatter path photographs for visibility of 30 miles

curves. As has been stated this is due to the fact that the power output of the LASER has a finite rise time which was not accounted for in the theory. Secondly, the slope of the real curves never becomes vertical because there is probably some degree of back-scatter at all distances due to secondary scattering effects, although the data obtained does not give a good indication of what happens at close range because of the small deflection of the oscilloscope trace at these ranges and the resultant large errors in measuring these deflections. Table II summarizes all the backscatter data photographs.

Determination of Signal Power

The signal return strength versus range was actually determined by measuring the signal return from only one target, the Hilltop Tank. To this measurement the inverse square law and an atmospheric attenuation correction were applied. The attenuation correction was the same as discussed in Chapter III. The reasons for using this method instead of a more direct approach follow. A more direct method would have been to measure the signal return from each of the four targets for several conditions of visibility. As has been noted, however, the visibility may vary widely, depending on the direction of observation. This factor along could easily mask the true results. The reflectances and shapes of the two more remote targets introduce still more unknowns. Regarding the closest target there is the problem of parallax which introduces another source

Table II

Summary of Backscattering Data Photographs

Photograph Pair	Sweep Speed (μs/cm)	Receiver Oscilloscope Sensitivity (Volts / cm)	Field of View (Milliradians)	Photomultiplier Load Resistance	Visibility Miles
108-109	20	5	0.9	100	20
110-111	20	5	0.5	500	20
112-113	20	5	0.5	500	20
114-115	20	5	0.5	500	20
118-119	20	1	0.13	1000	20
120-121	20	2	0.13	1000	20
144(b)-145(b)	20	5	0.9	100	50
146(b)-147(b)	20	5	0.9	100	50
148(a)-149(a)	20	5	0.9	100	50
148(b)-149(b)	20	5	0.9	100	50

of error. At this close range it is necessary to use the smallest of the available field stops, $\omega = 0.13$, to prevent overloading of the preamplifier. In this case, the receiver field of view covers a spot only about 3 1/2 inches in diameter at the tank. Since the transmitted beamwidth is 2 milliradians it covers a spot 4.6 feet in diameter. These two spots are separated by the distance between the receiving mirror center and the transmitting objective which is 2 feet. The result is that the two spots barely overlap. The intensity of the LASER beam is greatest near the center and falls off toward the periphery so that the signals from the 126 Tank are smaller than they should be. At the distance of the Hilltop Tank the overlap, though still not optimum, is much better. For the above reasons it was concluded that a more generally applicable result would be obtained by the method employed, particularly in view of the time limitations imposed on the project. If considerable amounts of data for various values of visibility could have been collected and reduced, it is quite possible that many of the unknowns noted above could have been eliminated. Three shots at the Hilltop Tank were made on a night when the visibility was unusually good---perhaps 50 miles. Under these conditions, the attenuation at the range of the Hilltop Tank was less than 0.5 decibel and is ignored. Figure 25 shows the three shots. The transmitted waveform amplitude is different in (c) because the oscilloscope sensitivity was changed. The

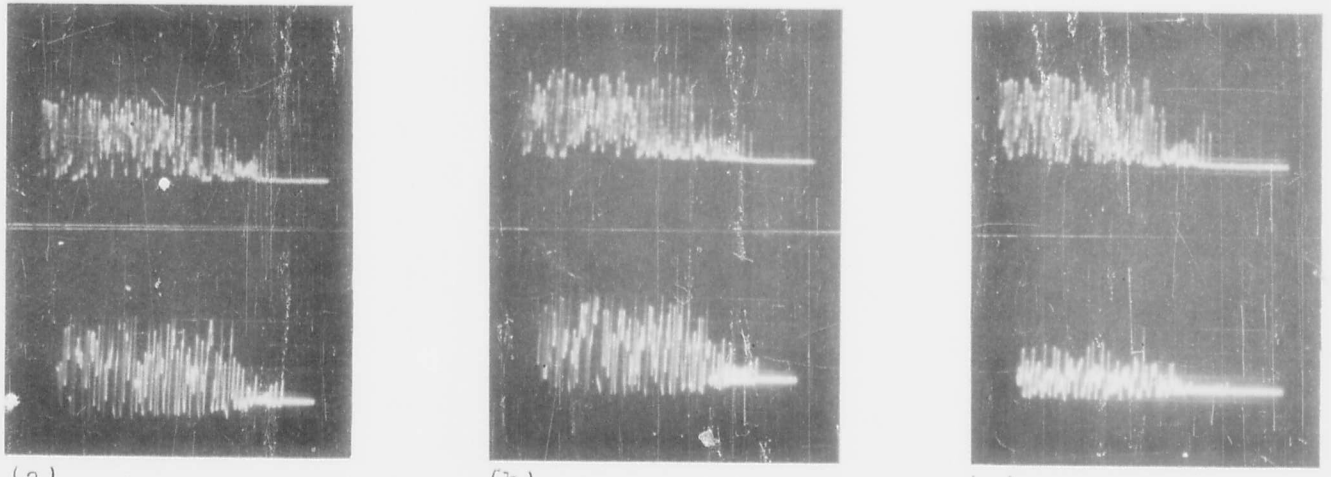

(a) (b) (c)

Top- Received signals
Bottom- Transmitted signals

$R_{\varphi} = 100; \omega = 0.13$; 5v/div.; 20μsec./div.

Fig. 25
Echo Signals from Milltop Theater Tank with Corresponding Transmitted Signals

results were quite consistent for the three shots as can be seen. The average peak amplitude of the signal was taken as being one-half the overall envelope height after power buildup was complete. This is somewhat arbitrary though partly based on the study of the LASER output envelope. For all three of the photographs presented, an average peak amplitude of 1.5 major divisions was assigned. Based on the nominal sensitivity of the photomultiplier, this is equivalent to 6.95×10^{-8} watts. Figure 26 is a plot of system response as a function of range and field of view in the absence of attenuation as projected from the above measurement. Figure 27 is a plot of the system response normalized to a field of view of 1 milliradian and corrected by the atmospheric attenuation data. The response at any other field of view may be found by multiplying by the square of the new field of view expressed in milliradians.

Signal-to-Noise-Ratio. The actual signal-to-noise-ratio was plotted in the same way as the predicted value. That is, the actual received signal corrected for atmospheric attenuation was compared with the average noise power and with the root-mean-square fluctuation of the noise power. These plots appear as Figures 28 and 29. Comparison of these with the corresponding predicted curves shows good agreement. The most significant difference is the difference between the day and night curves. According to the actual curves, the sunlight interference tends to be the dominant

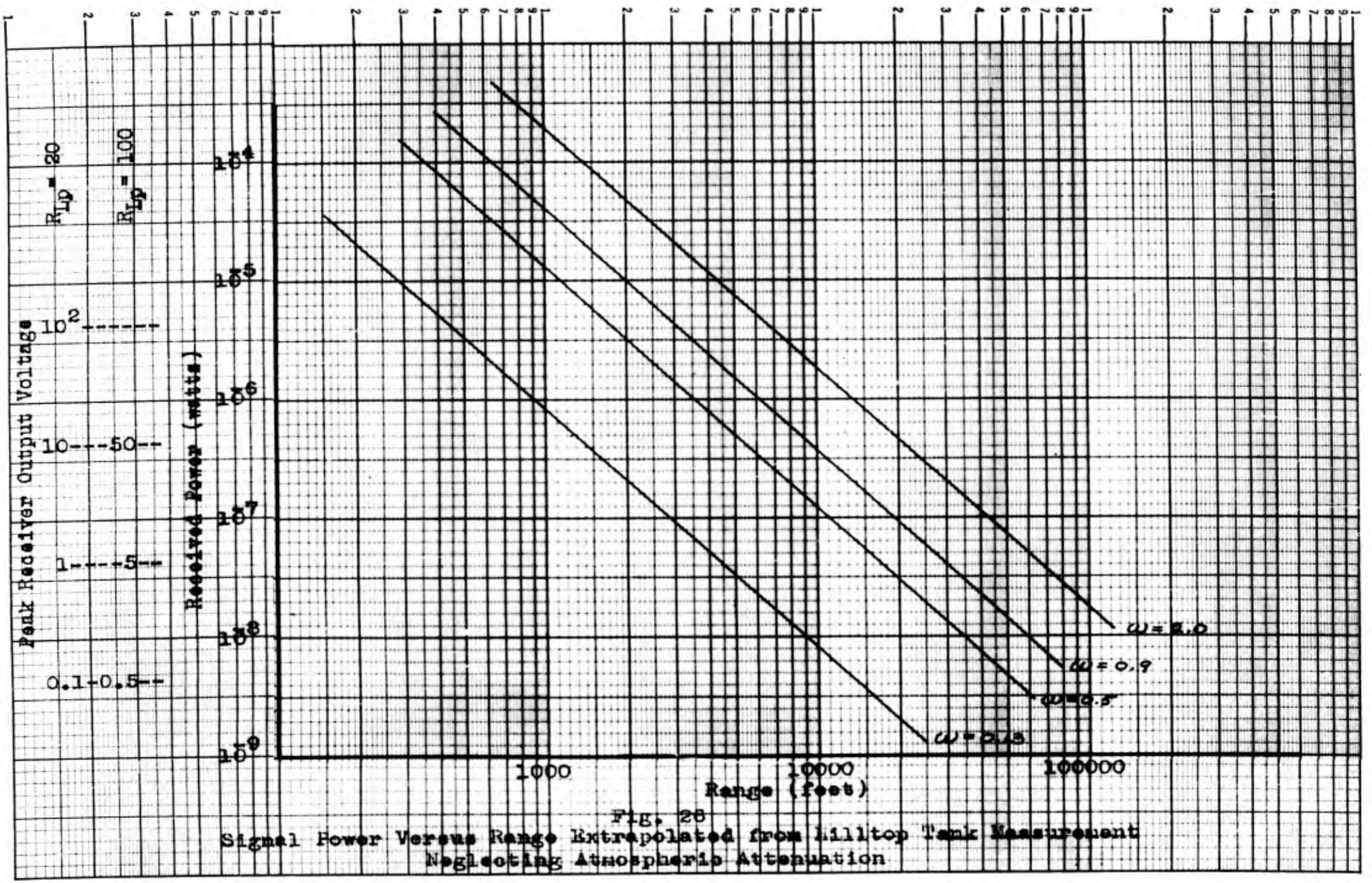

Fig. 26
Signal Power Versus Range Extrapolated from Hilltop Tank Measurement
Neglecting Atmospheric Attenuation

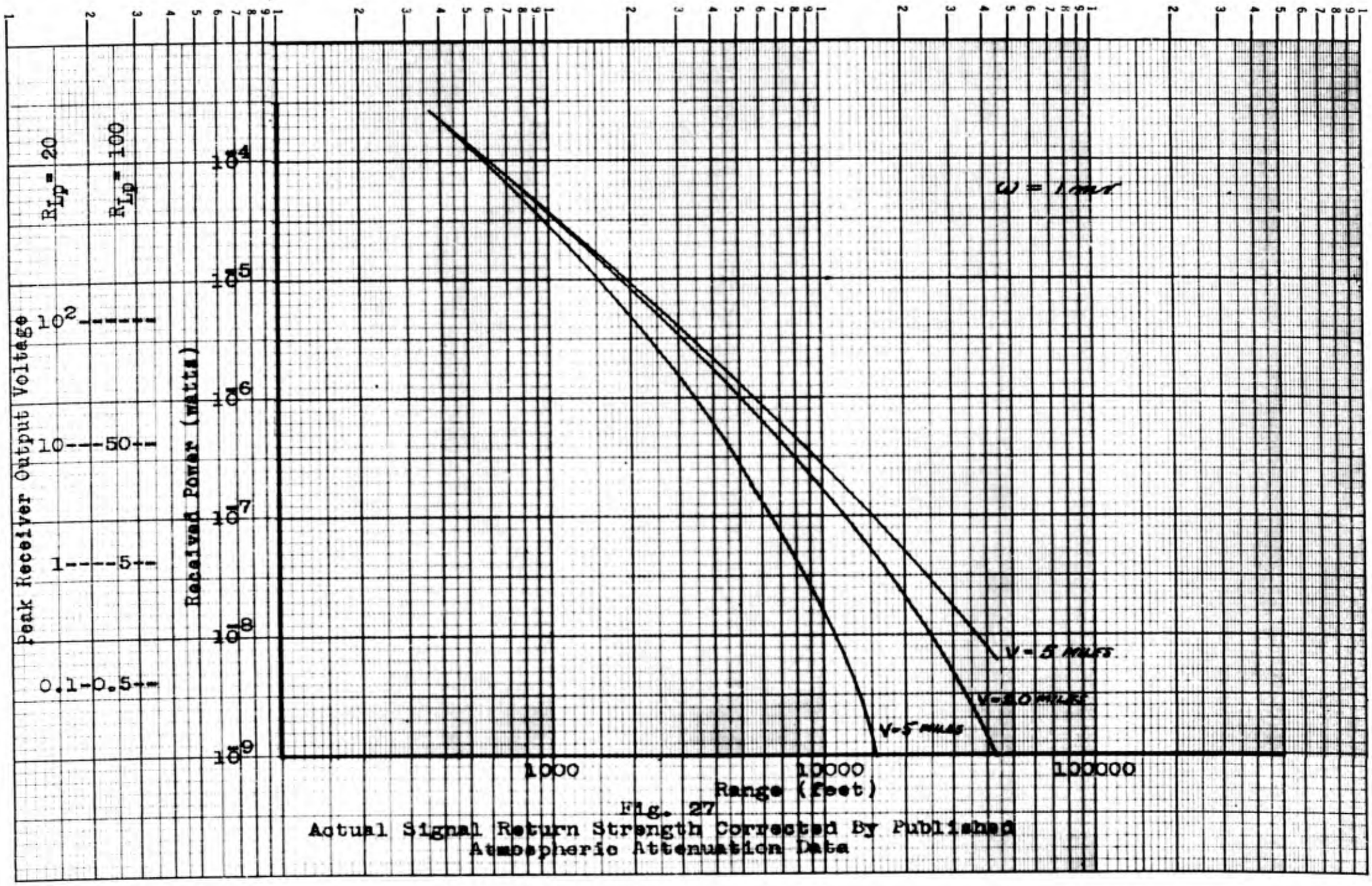

Fig. 27
Actual Signal Return Strength Corrected By Published Atmospheric Attenuation Data

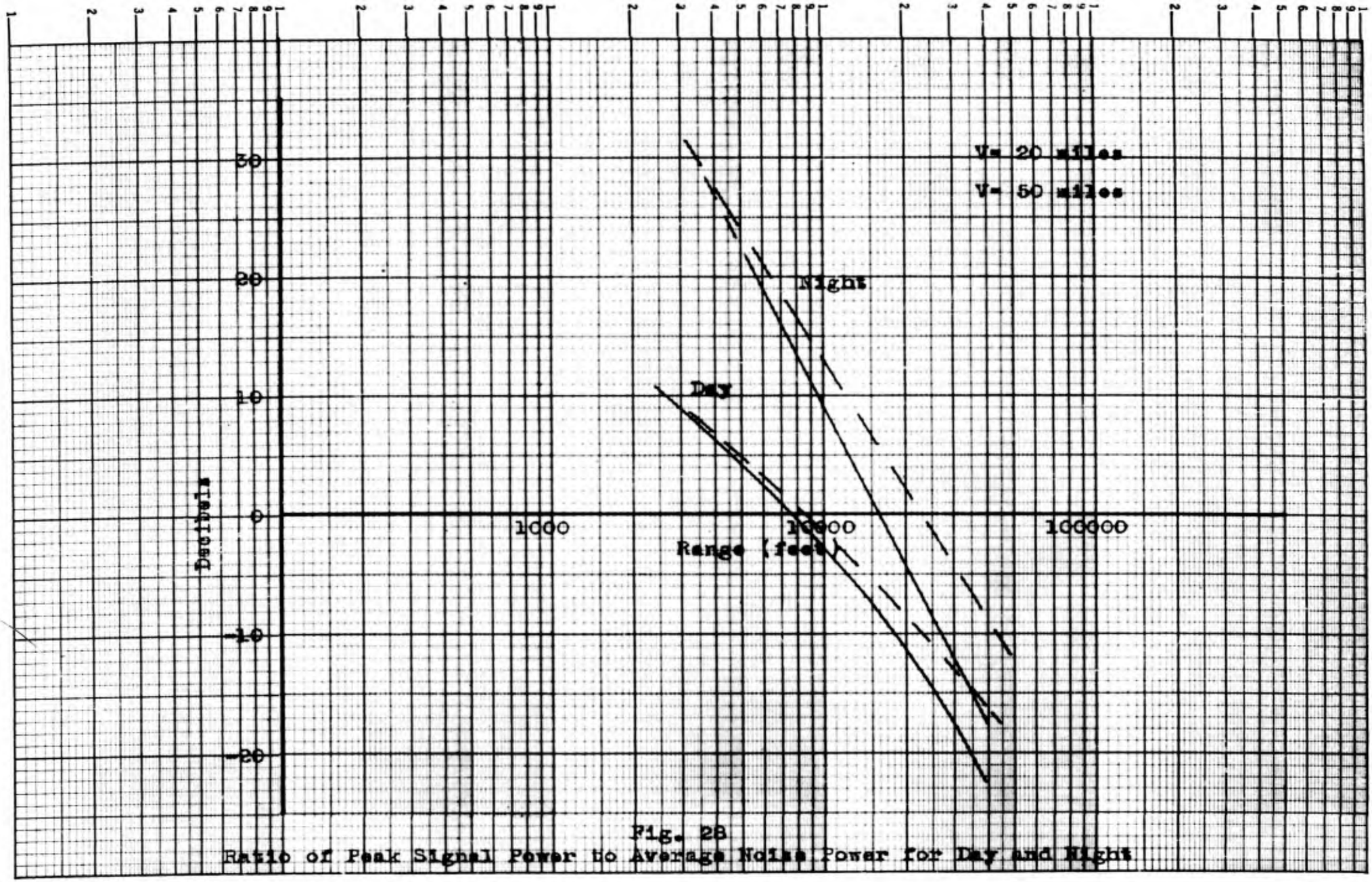

Fig. 28
Ratio of Peak Signal Power to Average Noise Power for Day and Night

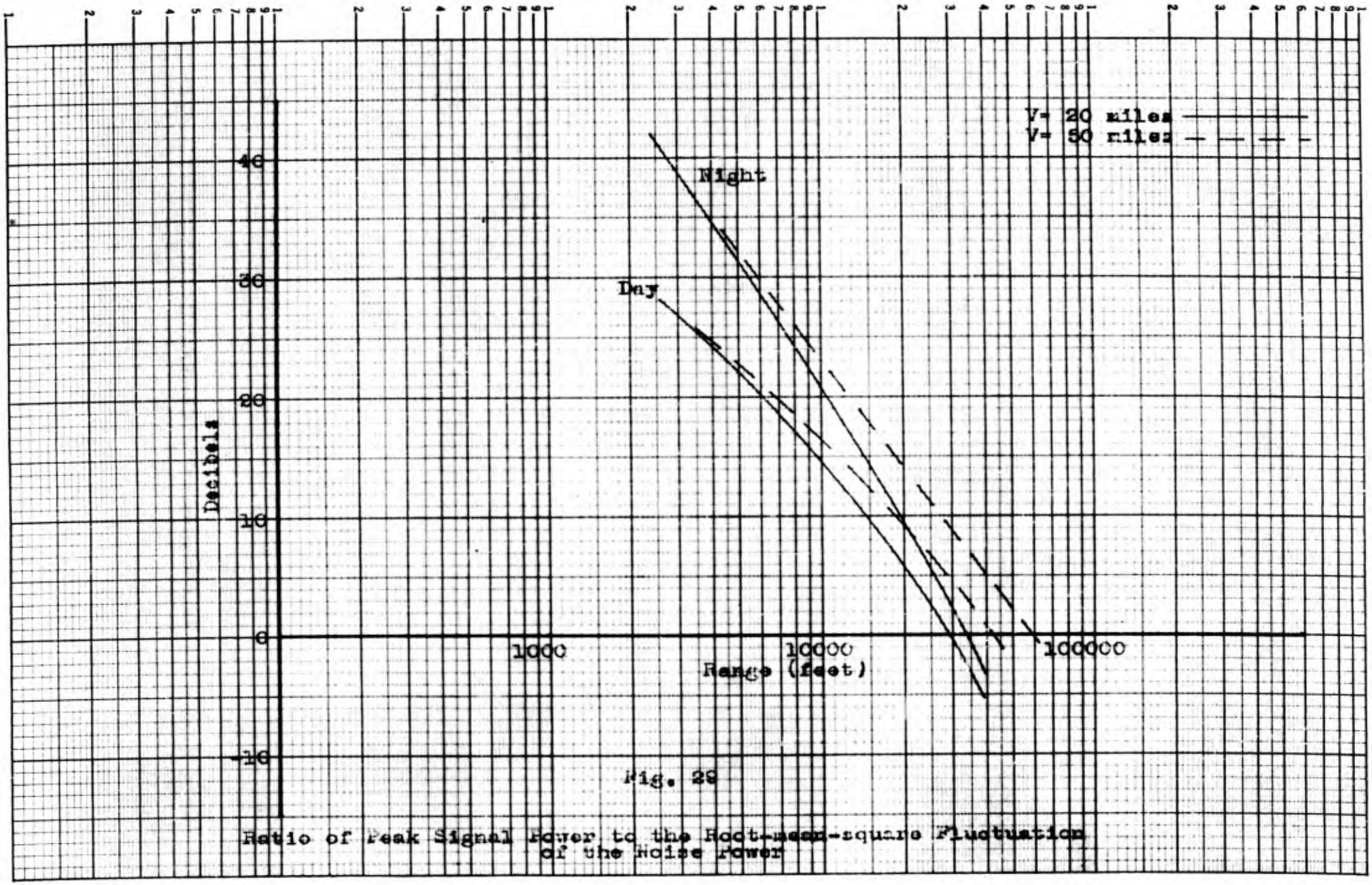

Fig. 28

Ratio of Peak Signal Power to the Root-mean-square Fluctuation of the Noise Power

noise as evidenced by the considerable difference between the day and night curves. For the predicted curves the reverse is true. The predicted curves would more nearly match the actual curves if a higher value of R_0 or a higher value of visibility had been assumed. This would also be true if a correction were made to the theory to account for the slow power buildup of the LASER.

Figure 18 on page 44 is a good illustration of the relationship between the signal and the root-mean-square noise fluctuation. The bottom trace which was made with the system pointed slightly away from the target shows the backscatter alone since the shot was made at night. The fluctuation is seen riding on top of the envelope. The top trace shows the echo from the target superimposed upon the backscatter. The manner in which the signal rides on top of the average backscattered power confirms qualitatively that the fluctuation is the actual interfering signal.

V. Conclusions and Recommendations

It is believed that the experimental results are quite indicative of the performance to be expected of the system regarding signal-to-noise-ratio as defined in the report. However, delays during the project arising from difficulties with the LASER equipment prevented the collection and reduction of the quantity of data that would be required to justify a great deal of quantitative confidence in the results.

The experimental results on the whole agree remarkably well with predictions. The limitations imposed by backscatter on an extended burst system were well illustrated and emphasize the need for a single high powered output pulse from the LASER for ranging applications.

It is recommended that if additional quantitative data is required, the following modifications be made to the equipment and methods:

1. A more accurate means of estimating visibility should be devised. The receiver itself might possibly be used in this connection---perhaps to determine contrast between distant objects and the sky
2. A means of monitoring the transmitter power output should be incorporated.

3. The sensitivity of the 7265 photomultiplier should be made variable, perhaps by varying its power supply voltage in order that large fields of view can be used in the daytime without damaging the tube.

Bibliography

1. Gray, Dwight E. American Institute of Physics Handbook. New York: McGraw-Hill Book Company, Inc., 1957.

2. Jahnke, Eugene and Fritz Emde. Tables of Functions. New York: Dover Publications, 1945.

3. Meyers, F.J. "Tactical Laser Radar Design." Interdepartmental Correspondence. Culver City, California: Hughes Aircraft Company, January 1961.

4. Middleton, W.E. Knowles. Vision Through the Atmosphere. Toronto, Canada: University of Toronto Press, 1952.

5. Oliver, B.M. "Some Potentialities of Optical Masers." Proceedings of the Institute of Radio Engineers, 50:135-141 (February 1962).

6. Rodda, S. Photo-electric Multipliers. London: MacDonald and Company, Ltd., 1953.

7. Sears, Francis W. Principles of Physics-Optics. Cambridge, Massachusetts: Addison-Wesley Press, Inc., 1948.

8. Smith, C.V. and M.L. Stitch. Applications of Lasers to Ranging and Tracking. Culver City, California: Hughes Aircraft Company (Aerospace Group), March 1962.

Appendix A

Derivation of Formula for Performance Without Attenuation or Interference

Figure 30 shows the geometry of the derivation. The transmitter beamwidth is γ and the receiving field of view is ω. If the transmitted power is P_t and the reflectance of the target is ρ, then assuming that the target intercepts the entire transmitted beam, the total reflected power is

$$P_t \rho \tag{14}$$

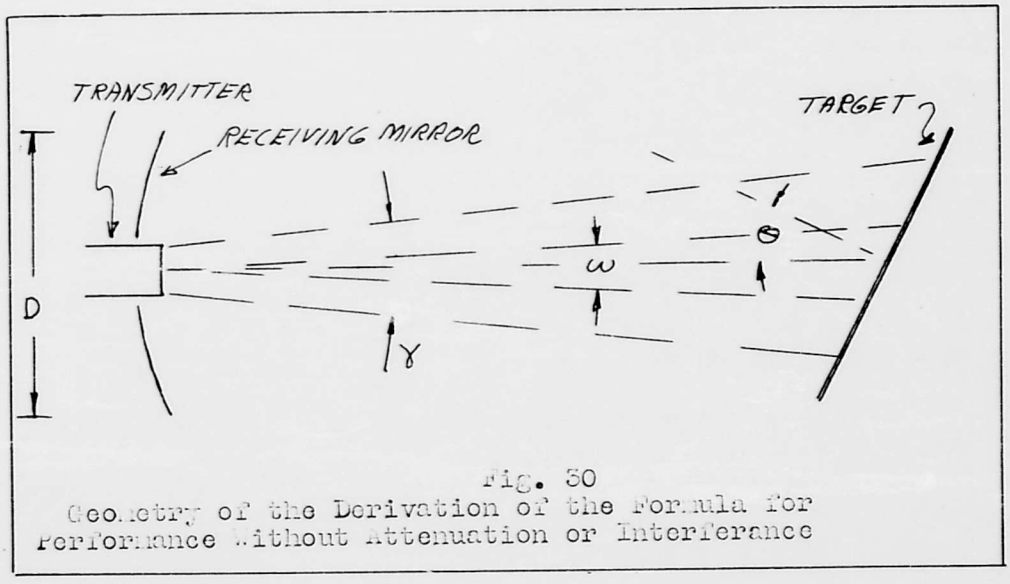

Fig. 30
Geometry of the Derivation of the Formula for Performance Without Attenuation or Interference

This total power is also the integral over the 2π steradians in front of the target of the radiant intensity (power per steradian) of the reflection. If the target is a diffuse reflector behaving according

to Lambert's cosine law, the radiant intensity of the reflected power is

$$I(\theta) = I_m \cos\theta \tag{15}$$

where I_m is the intensity perpendicular to the target. Integrating this expression yields

$$\int_0^{2\pi} I_m \cos\theta \, d\Psi = \pi I_m \tag{16}$$

where $d\Psi$ is the differential solid angle. Equating this to (14) and using (15) the radiant intensity of the reflection in the direction of the receiver is

$$I(\theta) = \frac{P_t \rho}{\pi} \cos\theta \qquad \begin{pmatrix}\text{power per solid} \\ \text{angle}\end{pmatrix} \tag{17}$$

The solid angle subtended by the receiving mirror is

$$\frac{\pi D^2}{4R^2}$$

so that the power received is

$$P_r = \frac{P_t \rho D^2 \cos\theta}{4R^2} \tag{18}$$

In the event that the receiver field of view is less than the transmitted beamwidth the above is reduced by the factor ω^2 / γ^2, the ratio of areas covered at the target. If n_r is the efficiency of the receiving optics the received power becomes

$$P_r = \frac{P_t \rho D^2 n_r \cos\theta}{4R^2} \left(\frac{\omega}{\gamma}\right)^2 \tag{19}$$

Appendix B

Derivation of Formula for Sunlight Reflected from the Target

Figure 31 shows the geometry of the derivation. Let the spectral irradiance of the sun at the target be H_s watts per unit

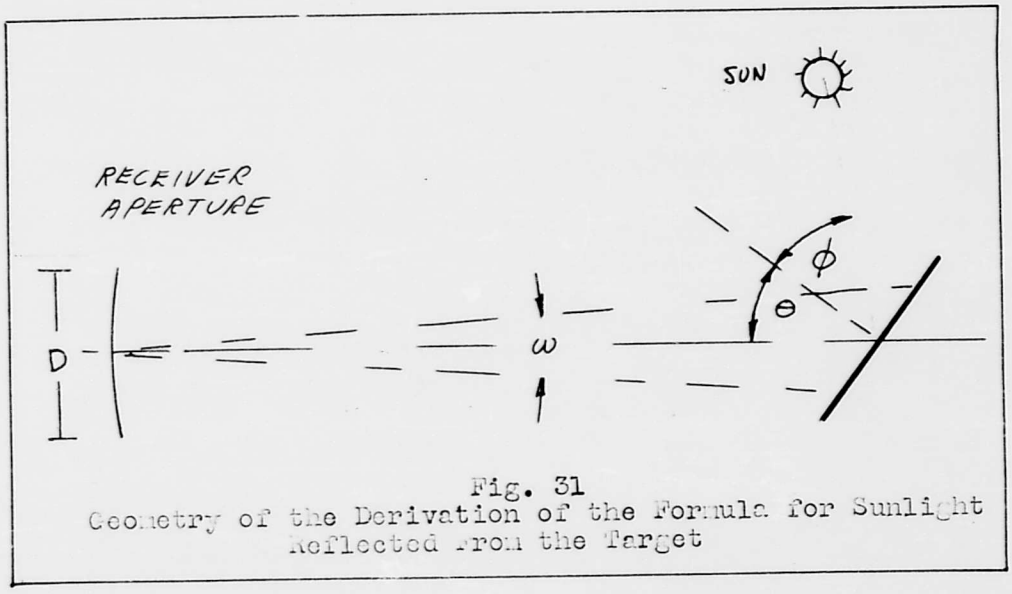

Fig. 31
Geometry of the Derivation of the Formula for Sunlight Reflected from the Target

area per $\mathring{A}$. Since the target is inclined with respect to the direction of the sun, the spectral irradiation (power per unit area per $\mathring{A}$ falling on the target) of the target is $H_s \cos \phi$. If the target has a reflectance ρ and an area A, the total reflected power per $\mathring{A}$ is:

$$H_s A \rho \cos \phi \qquad (20)$$

This total power may also be expressed as the integral over a hemisphere of the radiant intensity of the reflected energy. If the

target is assumed to be a diffuse reflector behaving according to Lambert's cosine law, the radiant intensity of the reflected energy may be expressed:

$$I(\theta) = I_m \cos\theta \quad \text{(watts)/(ster - Å)} \tag{21}$$

Integrating this over 2π steradians while assuming that the dimensions of the target are small compared to the distance between the target and receiver, the result is

$$\int_0^{2\pi} I(\theta)\, d\Psi = \pi I_m = H_S A \rho \cos\phi \tag{22}$$

where $d\Psi$ is the differential solid angle. Combining (21) and (22)

$$I(\theta) = \frac{H_S A \rho \cos\phi \cos\theta}{\pi} \quad \text{(watts) / (ster - Å)} \tag{23}$$

which is the intensity of the reflection in the direction of the receiver. The solid angle subtended at the target by the receiving aperture is

$$\frac{\pi \left(\frac{D}{2}\right)^2}{R^2} = \frac{\pi D^2}{4R^2} \quad \text{(steradians)} \tag{24}$$

so that the spectral sun power received is

$$S = \frac{\pi D^2}{4R^2} \; I(\theta) = \frac{D^2 H_S A \rho \cos\phi \cos\theta}{4R^2} \tag{25}$$

If the receiver field of view, ω, is smaller than the target, the area that the receiver actually views is

$$A = \pi \left(\frac{\omega R}{2}\right)^2 \sec\theta = \frac{\pi \omega^2 R^2}{4} \tag{26}$$

Substituting (26) into (25)

$$S = \frac{D^2 H_s \pi \omega^2 \rho \cos \phi}{16} \tag{27}$$

Finally, let B_o be the optical receiving bandwith, n_r the optical efficiency and T the transmission of the intervening atmosphere. Then the received power from the target becomes

$$P = \frac{\pi B_o T D^2 n_r H_s \omega^2 \rho \cos \phi}{16} \tag{28}$$

Letting $T = e^{-br}$ where b is the atmospheric attenuation constant

$$P = \frac{\pi B_o e^{-br} D^2 n_r H_s \omega^2 \rho}{16} \tag{29}$$

Appendix C

Derivation of Formula for Sunlight Scattered into Receiver by Atmosphere

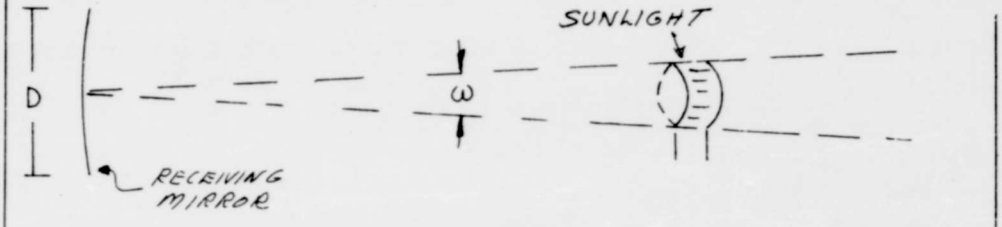

Fig. 32
Geometry of the Derivation of the Formula for Sunlight Scattered Into the Receiver by the Atmosphere

The elemental volume shown in Figure 32 has a volume

$$\frac{\pi}{4} (\omega r)^2 \, dr \tag{30}$$

Let H_S be the spectral irradiance of the sun and B' the volume scattering coefficient. The volume scattering coefficient is the power per steradian scattered in a given direction per unit volume of the atmosphere per unit incident power per unit area. Assume that the scattering of sunlight by the atmosphere is isotropic. Then

by definition of B' the spectral power per steradian scattered in all directions is (Ref 4:16)

$$H_S \cdot \frac{\pi}{4} (\omega r)^2 \, dr \cdot B' \tag{31}$$

In traveling to the receiver, the spectral power from each element of the cone suffers an inverse square loss and an attenuation loss. If the optical filter bandwidth B_0 is also introduced at this point, the power entering the receiver due to an element of the receiving cone is

$$\pi \frac{D^2}{4} B_0 H_S B' \frac{\pi}{4} (\omega r)^2 \frac{e^{-br}}{r^2} \, dr \tag{32}$$

where b = constant of attenuation due to scattering.

Integrating over the cone from the receiver to the target the total power is

$$D^2 B_0 H_S B' \frac{\pi^2}{16} \omega^2 \int_0^R e^{-br} \, dr = \frac{D^2 B_0 H_S B' \pi^2 \omega^2}{16 b} (1-e^{-br}) \tag{33}$$

The volume scattering coefficient B' is related to the attenuation constant b in the case of isotropic scattering by $B' = b/4\pi$ (Ref 5:17). Therefore, the total received power assuming a receiving optics efficience of n_r is:

$$\frac{n_r D^2 B_0 H_S \pi \omega^2}{64} (1 - e^{-br}) \tag{34}$$

Appendix D

Derivation of Formula for Backscattering

of Laser Power into Receiver by Atmosphere

(Based on Reference 3)

Assume: (1) absorption by the atmosphere is negligible

(2) atmosphere is uniform

(3) intensity of LASER beam is constant over its crossection

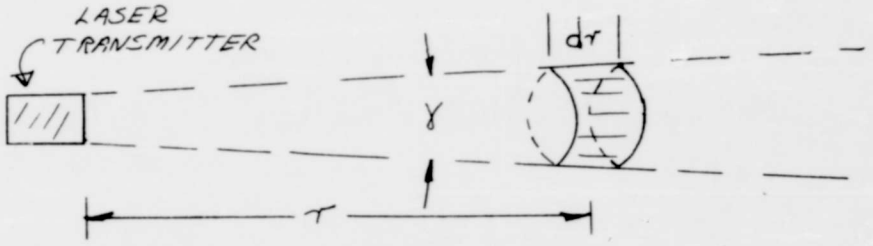

Fig. 33
Geometry of the Derivation of the Formula for
Backscattering of LASER Power into the Receiver

If P_t is the transmitted power, then the power incident on the infinitesimal volume shown in Figure 33 is

$$P(r) = P_t e^{-br} \tag{35}$$

where b = constant of attenuation due to atmospheric scattering - (total scattered power per unit incident power per unit length of the beam).

A part of this power is scattered back in the direction of the receiver. Specifically the intensity of the backscatter from the beam element is:

$$dI_r = B\,P(r)\,dr = B\,P_t\,e^{-br}\,dr \quad \left(\frac{\text{power}}{\text{steradian}}\right) \tag{36}$$

where B = scattering coefficient for back-scatter (power per steradian per unit incident power per unit length of the beam)

B and b are related. In fact, if the scattering of the beam were isotropic then $b = 4\pi B$ since b is associated with the total scattering over 4π steradians. According to Meyers (Ref 3) there is theoretical and experimental justification for assuming that B is only half the isotropic value so that $B = b/8\pi$. The constant b may be related to the meteorological visibility in order that its value may be estimated from visual observation. Meteorological visibility is defined as that distance at which a large dark object is barely visible against a daylight horizon. The human eye requires a 2% contrast for detectability. Therefore, under these conditions, 98% of the light seen by an observer looking at the horizon originates between the object and the observer and only 2%, therefore, from beyond the object. This is equivalent to stating that light originating at the object is attenuated by 98%. Therefore, in terms of symbols used previously

$$\frac{P(r)}{P_t} = e^{-bV} = 0.02 \tag{37}$$

and

$$b = \frac{3.92}{V} \tag{38}$$

Therefore, b and B are known in terms of the meteorological visibility.

Returning to equation (36) and noting that the intensity of backscattering will suffer an additional attenuation on its return path equal to that on the outgoing path and also that it will suffer an inverse square loss in returning to the receiver, the following is obtained:

$$d I_r = \frac{B P_t e^{-br} dr}{r^2} \tag{39}$$

If the receiving aperture has diameter D then the differential power received is

$$d P_r = \frac{\pi B D^2 P_t}{4} \frac{e^{-br} dr}{r^2} \tag{40}$$

The receiver field of view overlaps the transmitted beam beginning at a distance R_0 from the system depending on the separation of the two. To obtain the total backscattered power received (40) is integrated from R_0 to R_t, the target distance. This integration yields:

$$P_r = \frac{\pi B D^2 P_t}{4} \left(-2 b E_i (-2 br) - \frac{1}{r} e^{-2br} \right)_{R_0}^{R_T} \tag{41}$$

where R_0 and R_t are indicated as limits of integration in the equation and

$$E_i (-x) = -\int_x^{\infty} \frac{e^{-t}}{t} dt \tag{42}$$

may be evaluated by the use of Reference 2.

Vita

Alton Bernard Todd was born on [redacted] in [redacted], the son of John Norton Todd, Jr. and Edith [redacted] Key. After completing his work in [redacted], he attended North Georgia College, Dahlonega, Georgia, under the Army Specialized Training Reserve Program. In April 1945, he went on active duty in the Army Air Corps. After discharge from the Army in November of the same year, he entered Alabama Polytechnic Institute, Auburn, Alabama and received the degree of Bachelor of Electrical Engineering in December, 1948. In February, 1949, he accepted a position as an Electronic Engineer at Wright-Patterson Air Force Base where he worked until coming to the Air Force Institute of Technology.

Permanent Address: [redacted]

This Thesis was typed by Mrs. Jack E. Hesse, Jr.